AD-A111 828 PHYSICAL SCIENCES INC WOBURN MA F/G 17/5
DEVELOPMENT OF COCHISE UV ABSORPTION SYSTEM,(U)
DEC 81 L G PIPER, H C MURPHY, W T RAWLINS F19628-80-C-0174
UNCLASSIFIED PSI-TR-292 AFGL-TR-81-0318 NL

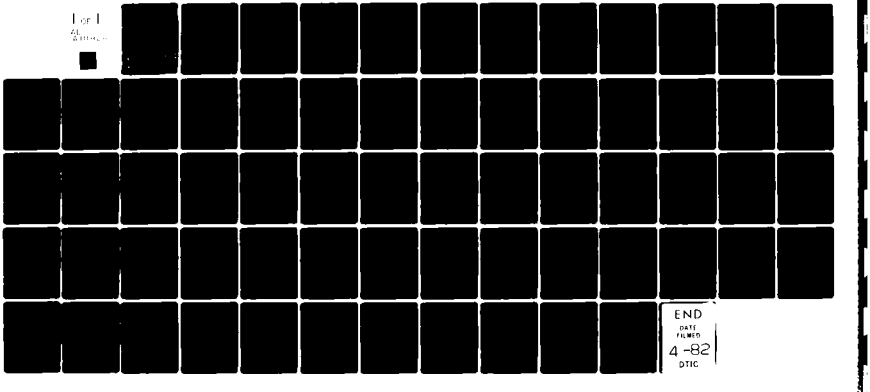

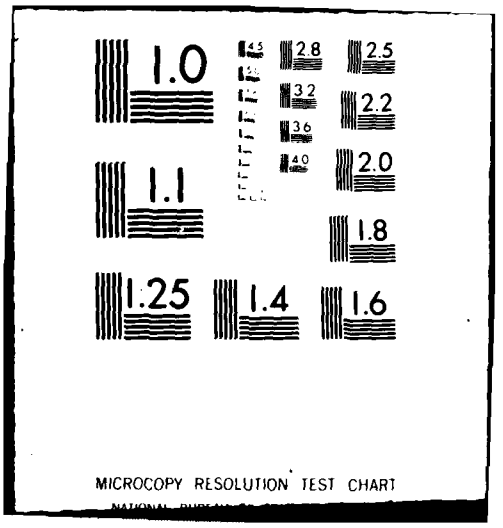
1.0
1.1
1.25
1.4
1.6
1.8
2.0
2.2
2.5
2.8
3.2
3.6
4.0
MICROCOPY RESOLUTION TEST CHART

(12)

AFGL-TR-81-0318

# DEVELOPMENT OF COCHISE UV ABSORPTION SYSTEM

L.G. Piper
H.C. Murphy
W.T. Rawlins

Physical Sciences Inc.
30 Commerce Way
Woburn, Massachusetts 01801

Final Report
7 July 1980 - 30 October 1981

December 1981

Approved for public release; distribution unlimited



AIR FORCE GEOPHYSICS LABORATORY
AIR FORCE SYSTEMS COMMAND
UNITED STATES AIR FORCE
HANSCOM AFB, MASSACHUSETTS 01731

UNCLASSIFIED

SECURITY CLASSIFICATION OF THIS PAGE (When Data Entered)

| REPORT DOCUMENTATION PAGE | | READ INSTRUCTIONS BEFORE COMPLETING FORM |
|---|---|---|
| 1. REPORT NUMBER<br>AFGL-TR-81-0318 | 2. GOVT ACCESSION NO.<br>AD-A111228 | 3. RECIPIENT'S CATALOG NUMBER |
| 4. TITLE (and Subtitle)<br>DEVELOPMENT OF COCHISE UV ABSORPTION SYSTEM | | 5. TYPE OF REPORT & PERIOD COVERED<br>FINAL REPORT<br>07/07/80-30/10/81 |
| | | 6. PERFORMING ORG. REPORT NUMBER<br>PSI TR-292 |
| 7. AUTHOR(s)<br>L. G. Piper, H. C. Murphy and W. T. Rawlins | | 8. CONTRACT OR GRANT NUMBER(s)<br>F19628-80-C-0174 |
| 9. PERFORMING ORGANIZATION NAME AND ADDRESS<br>Physical Sciences Inc.<br>30 Commerce Way<br>Woburn, MA 01801 | | 10. PROGRAM ELEMENT, PROJECT, TASK AREA & WORK UNIT NUMBERS<br>61102F<br>2310G4AR |
| 11. CONTROLLING OFFICE NAME AND ADDRESS<br>Air Force Geophysics Laboratory<br>Hanscom AFB, Massachusetts 01731<br>Monitor/Russell Armstrong/OPR | | 12. REPORT DATE<br>December 1981<br>13. NUMBER OF PAGES<br>64 |
| 14. MONITORING AGENCY NAME & ADDRESS(if different from Controlling Office) | | 15. SECURITY CLASS. (of this report)<br>UNCLASSIFIED<br>15a. DECLASSIFICATION/DOWNGRADING SCHEDULE |

16. DISTRIBUTION STATEMENT (of this Report)

Approved for public release; distribution unlimited.

17. DISTRIBUTION STATEMENT (of the abstract entered in Block 20, if different from Report)

18. SUPPLEMENTARY NOTES

19. KEY WORDS (Continue on reverse side if necessary and identify by block number)

Resonance absorption
Metastable nitrogen atoms
Discharge line sources
Vacuum ultraviolet techniques
Plasma excitation mechanisms

20. ABSTRACT (Continue on reverse side if necessary and identify by block number)

Under this program PSI developed a resonance lamp to be used to measure number densities of $N(^2D)$ and $N(^2P)$ in the COCHISE facility using the technique of vacuum ultraviolet resonance absorption. The lamps consist of sapphire tubes through which argon containing a trace of molecular nitrogen flows. A low power microwave discharge through the gas excites the VUV resonance lines which are diagnostic of the atomic nitrogen metastables (149.3 nm for $N(^2D)$ and 174.3 nm $N(^2P)$. An interference filter is

DD FORM 1 JAN 73 1473 EDITION OF 1 NOV 65 IS OBSOLETE

UNCLASSIFIED

SECURITY CLASSIFICATION OF THIS PAGE (When Data Entered)

20. ABSTRACT CONTINUED

used to isolate the appropriate resonance multiplet, and the radiation, after traversing the COCHISE reaction zone twice, is detected with a solar-blind photomultiplier.

The major lamp-design criterion is dictated by the important excitation mechanisms in the lamp. VUV resonance-line excitation mechanisms are discussed in detail, and experimental methods for elucidating these mechanisms are presented.

TABLE OF CONTENTS

LIST OF FIGURES

# 1. INTRODUCTION

Under this program PSI developed a resonance lamp to be used to measure number densities of $N(^2D)$ and $N(^2P)$ in the COCHISE facility[1] using the technique of vacuum ultraviolet resonance absorption. The lamps consist of sapphire tubes through which argon containing a trace of molecular nitrogen flows. A low power microwave discharge through the gas excites the VUV resonance lines which are diagnostic of the atomic nitrogen metastables (149.3 nm for $N(^2D)$ and 174.3 nm $N(^2P)$). An interference filter is used to isolate the appropriate resonance multiplet, and the radiation, after traversing the COCHISE reaction zone twice, is detected with a solar-blind photomultiplier.

We have discussed in detail previously the criteria important in designing VUV resonance lamps,[2] and have presented papers on the subject at the Technical Symposium East '81 of the Society of Photo-Optical Instrumentation Engineers[3] and at the 34th Gaseous Electronics Conference.[4] The important issues are the sensitivity of the diagnostic, the ease of implementation of the diagnostic, and whether or not the sensitivity of the diagnostic changes with temperature. The sensitivity of the diagnostic and its temperature dependence both are controlled by the mechanisms within the lamp which govern emission-line excitation. Lamps filled with helium bath gas are excited by electron-impact collisions, whereas those with argon bath gas are excited in the transfer of energy between metastable argon atoms and ground-state nitrogen atoms. Since the exoergicity of the energy-transfer is somewhat larger than the prevailing kinetic temperature in typical low-power-microwave resonance lamps, the translational temperature of the excited nitrogen atoms produced in the energy-transfer reaction will be somewhat greater than that from atoms excited by electron impact. Thus the emission lines in the argon lamp will be broader than in the helium lamp with a concomitant decrease in the sensitivity of the absorption diagnostic in the argon lamp.

The prevailing kinetic temperature in a microwave lamp in a room temperature environment can be determined by measuring the rotational temperature of OH emissions when a little $H_2O$ has been added to the discharge. At room temperature, typical plasma temperatures are about 500 K in a 12 mm diameter

lamp operated with about 20 watts of discharge power. The lamp kinetic temperature will be less in the cold environment of the COCHISE facility, but the extent of cooling cannot be determined easily.

The exoergicity of the energy-transfer reaction between metastable argon atoms and ground-state nitrogen atoms is unaffected by changes in ambient temperature. Thus the effective kinetic temperature of the excited nitrogen atoms in an argon lamp should remain constant in cooling the lamp from 300 K to 80 K. Therefore, even though the sensitivity of the argon lamp is somewhat less than that of the helium lamp, the uncertainty in the calibration carried out on a room temperature facility should be much less in an argon lamp at 80 K than for a helium lamp at 80 K. We chose to build an argon lamp for the COCHISE measurements because the calibration should be unaffected by cooling. In addition, the argon lamp is easier to implement in COCHISE because no additional plumbing is required to exhaust the gas flowing through the discharge lamp.

In the following sections of this report, we will describe the absorption diagnostic that we have built and discuss its operating characteristics including an estimate of the sensitivity of the diagnostic. We also will discuss some of the calibration experiments which we ran on the FAKIR facility. In Appendix A we present a complete text of the paper given at the SPIE meeting which describes in detail the theory of resonance line absorption, the various sources of resonance-line broadening in VUV line sources, and the experimental facility used in these experiments. In Appendix B we have compiled drawings of components of the VUV diagnostic which we delivered to the Air Force Geophysics Laboratory in September, 1981.

## 2. DESCRIPTION OF COCHISE VUV RESONANCE LAMP

The immediate purpose of the vacuum-ultraviolet (VUV) resonance absorption diagnostic for the COCHISE apparatus is to measure the absolute concentrations of $N(^2D)$ and $N(^2P)$ in the reaction zone in order to relate those quantities to the NO infrared chemiluminescence observed in the reaction of active nitrogen with oxygen.[5] Establishing a working diagnostic for these species will allow longer range development of similar diagnostics for other atomic species such as $N(^4S)$, $O(^3P)$, and $H(^2S)$.

The metastable species $N(^2D)$ and $N(^2P)$ absorb radiation from their resonance multiplets at 149 nm and 174 nm, respectively.[6,7] In this section we outline how this method is to be applied to the COCHISE experiment. We present the general design of the optical system, review briefly the resonance absorption method, and examine the sensitivity of this application.

The VUV diagnostic PSI has built for COCHISE uses the optical configuration illustrated in Fig. 1. Radiation from a resonance-line source mounted on the IR mirror flange is directed through the center of the reaction cell, reflected from a plane $MgF_2$-coated mirror mounted on the IR lens baffle, and viewed by a solar-blind photomultiplier tube located on the IR mirror flange. Baffles on the source and detector eliminate scattered light. The line source is a simple flow system in which the NI resonance radiation is excited by a microwave discharge through 1-5 torr of Ar containing trace amounts of $N_2$;[3,6] the design criteria for the line source are discussed further in Appendix A. A $MgF_2$ window isolates the line-source gas from the reaction cell. The temperatures of the line source, mirror, and filters will be monitored and controlled by Pt resistance thermometers and resistance heaters similar to those now in use at numerous locations throughout the apparatus. Design drawings of the lamp components are in Appendix B.

The diagnostic configuration for COCHISE samples symmetrically through the center of the reaction zone, and does not compromise the infrared detection system. Using a monochromator to separate the $N(^2D)$ and $N(^2P)$ resonance

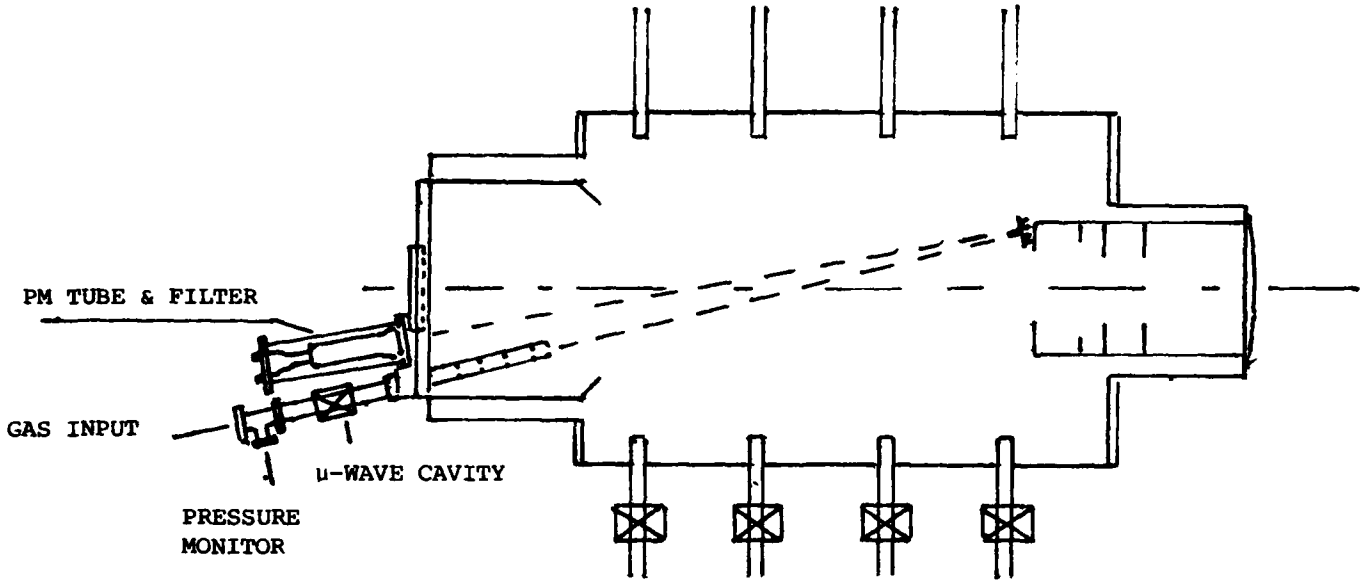


Fig. 1 Schematic view of COCHISE reaction cell modified for VUV absorption experiments.

1"

1/8 scale

multiplets as in conventional experiments is impractical in the COCHISE application. Thus appropriate filters are used to isolate the desired multiplets. The N($^2$P) 174 nm multiplet can be isolated from features at longer and shorter wavelengths by a suprasil window ($\lambda$ > 160 nm) coupled with a solar-blind photomultiplier tube ($\lambda$ < 190 nm). The N($^2$D) 149 nm multiplet can be separated from the 174 nm lines and from the OI 130 nm triplet (which may also be produced by the line source) using a special dielectric-stack coating upon a high-grade quartz or $MgF_2$ substrate. The latter filter is an adaptation of a UV-laser-reflector coating;[8] the coating in this case is designed to reflect at 174 nm, and transmit at 149 nm. Similar filters have been used successfully in resonance fluorescence measurements of N($^2$D) and N($^2$P) in a conventional discharge-flow system.[9]

The low temperatures in COCHISE will affect the transmission characteristics of the substrate and coating. The rate of temperature change during cooldown and warmup of the COCHISE facility is rather slow, so that the integrity of the filters will not be affected seriously by routine temperature cycling of the hardware. However, the short-wavelength cutoffs of common UV-window materials shift toward the blue when the temperature is reduced,[10] and the transmission window of the multilayer coating probably behaves in a similar manner. Therefore, the desired operating temperature of the filters must be known to establish design points for their fabrication.

The theory of line absorption is treated in detail in Section 2 of Appendix A. Because the resonance lines emitted from the lamp are actually multiplets, the calculated absorption will be the weighted sum of the absorption of the individual lines:

$$A_{tot} = \frac{\sum_i I_i A_i (k_{oi}\ell)}{\sum_i I_i} \qquad (1)$$

where $I_i$, $A_i$ and $k_{oi}\ell$ are the intensity, fractional absoprtion and optical depth of component i. The optical depths of the lines in the multiplet will differ because of differences in oscillator strength and ground-state

degeneracy between the components of the multiplet. Because both the absorption and emission line shapes are determined by Doppler broadening, the critical parameter in determining the sensitivity of the absorption diagnostic is the ratio of the effective kinetic temperature of the emission line to that of the absorption line:

$$\alpha^2 = \frac{T_{emitter}}{T_{absorber}} \tag{2}$$

A useful equation for calculating line absorptions is:

$$A = \frac{I_o - I}{I_o} = \sum_n \frac{(-1)^{n-1} (k_o \ell)^n}{n! \left(1 + n\alpha^2\right)^{1/2}} \quad . \tag{3}$$

where $I_o$ and I are incident and transmitted line intensities, respectively. Usually only the first two to three terms are significant for low optical depths ($k_o \ell \lesssim 0.1$).

The calibration experiments described in Section 3 show that in an argon lamp the effective kinetic temperature of the $N^*(3s\ ^2P)$ emitters is $\approx$ 4000 K. The absorbing $N(^2D)$ atoms in COCHISE have a kinetic energy $\approx$ 100 K, so that $\alpha \approx 6.3$ is appropriate for absorbance calculations in COCHISE using an argon lamp.

We estimate a minimum detectable absorption of about 0.005 which corresponds to an average $N(^2D)$ optical depth of 0.05 for $\alpha = 6.3$ and a COCHISE path length of 110 cm. This optical depth corresponds to a minimum detectable $N(^2D)$ number density of $1.1 \times 10^9$ atoms $cm^{-3}$. We expect number densities in COCHISE 4-5 times larger than this value; thus the sensitivity is adequate for the proposed measurements. Using a helium lamp will improve sensitivity towards $N(^2D)$ by a factor of two or three, but at the cost of significant calibration uncertainty as discussed above.

## 3. CALIBRATION EXPERIMENTS

We measured the absorption of various number densities of $N(^2D)$ from argon lamps as a function of lamp pressure and applied power, and compared these measurements to helium-lamp measurements for which the emission-line profile is expected to be determined by the prevailing kinetic temperature in the lamp. We also measured the kinetic temperature in the lamp both with thermocouple-probe measurements and with measurements of the rotational temperature of $OH(A\ ^2\Sigma^+)$ in the lamp when small amounts of water were added to the helium or argon bath gas. The thermocouple measurements were consistently higher than the OH rotational-temperature measurements, but generally showed the same variations with pressure and forward power. We didn't expect the thermocouple-probe to be accurate for absolute temperature measurements because the probe could be heated by microwave absorption, electron or ion bombardment, catalitic recombination of atoms or de-excitation of metastables. In addition the probe measurements indicated large axial and radial temperature gradients. Whereas the probe samplied a small volume in the center of the discharge region, the OH rotational measurements were averages over a large and extended volume.

The absorption measurements showed a decrease in sensitivity of a factor of 2.2 in changing from helium to argon lamps. This difference is close to what would be expected based upon the known exoergicity of the $Ar^*(^3P_2) + N$ energy-transfer reaction. The data showed only a weak pressure dependence, with the effective emission linewidth being slightly broader at lower pressures. The effective emission linewidth determined from the data was essentially independent of discharge power except at extreme low and high power.

### 3.1 Rotational Temperature Measurements

Traces of water were added to the lamp gas by bubbling the rare gas at high pressure (≈ 12 psig) through distilled water maintained at 0°C by an ice bath. The partial pressure of water in the discharge region was then ≈ 5-10 mtorr compared to a total gas pressure of ≈ 2 torr. With water vapor in the gas, the discharge excited the OH $[A\ ^2\Sigma^+(v'=0) - X\ ^2\pi(v''=0)]$ transition at 308 nm quite strongly (see Fig. 2). The 0.5 m Minuteman monochromator was just barely capable of resolving the several rotational lines in the $Q_1$-branch and the S-branch when operated with 50 μm slits in the third order using a 1200 g/mm grating blazed at 250 nm.

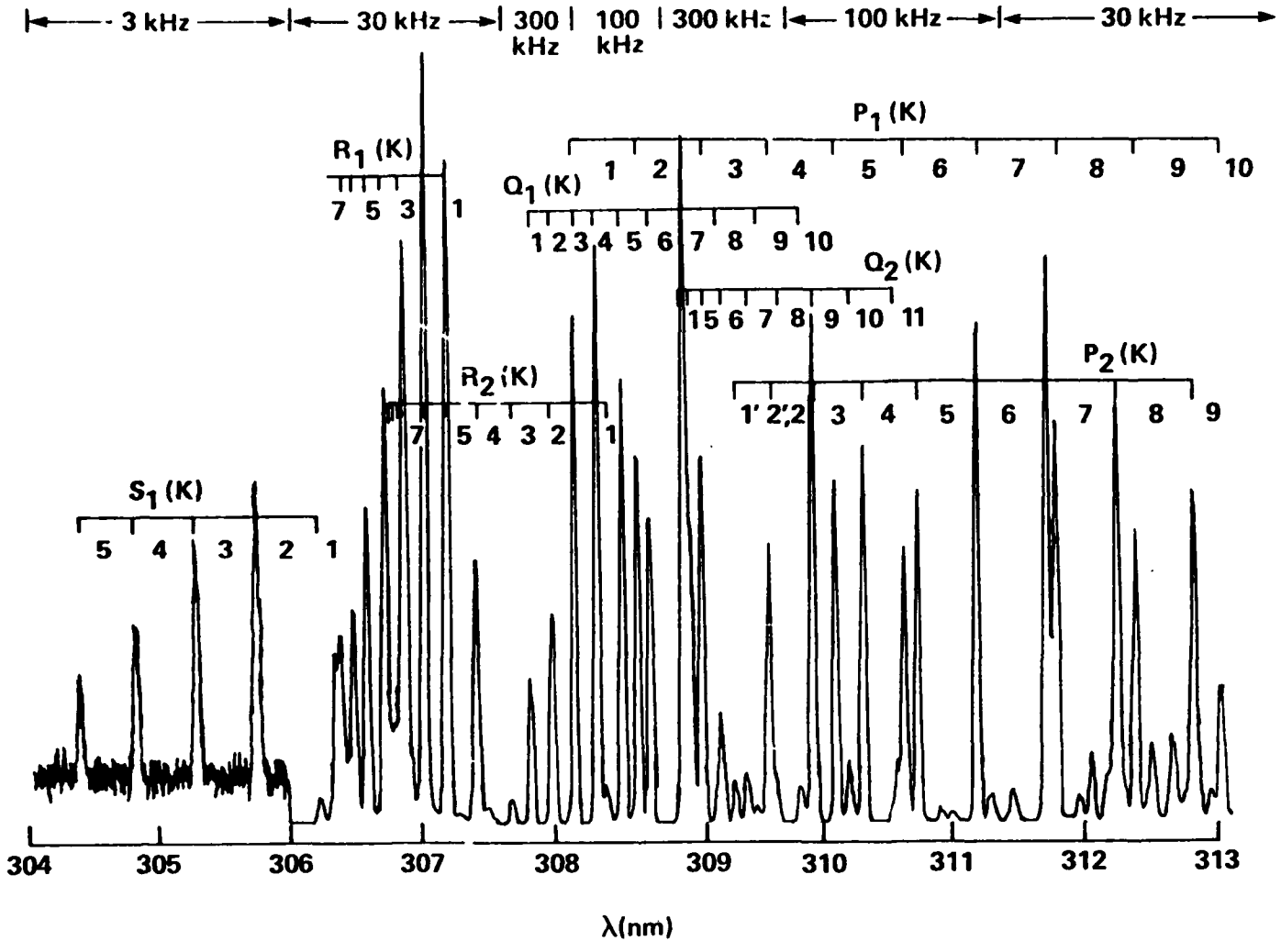


Fig. 2 A portion of the OH[$A^2\Sigma^+(v'=0)$] - $X^2\pi(v''=0)$ emission spectrum excited in a 2 torr 100 watt He/$H_2O$ lamp ($X_{H_2O}\approx 0.003$). Some of the many rotational branches are marked on the figure as are the relative intensities of the spectral lines.

The emission intensities from the rotational levels are proportional to the population and transition probability of the level being observed. If the rotational levels in the emitting state are in Boltzmann equilibrium we have $I_{v''J''}^{v'J'} \propto (2J'+1)\, A_{v''J''}^{v'J'}\, N_{v'}\, e^{-E_{v'J'}/kT}$. Thus semilog plots of the quantity $\ln I_{v''J''}^{v'J'}/(2J'+1)A_{v''J''}^{v'J'}$ versus $E_{v'J'}$ should be linear with a slope equal to $1.4388/T$ for energies in $cm^{-1}$. We used relative $A_{v''J''}^{v'J'}$ values of Chidsey and Crosley.[11]

Several representative plots are shown in Figs. 3 and 4. Figures 5, 6, and 7 show plots of temperature versus lamp pressure and discharge forward power for both $Q_1$-and S-branch measurements and for the thermocouple measurements. The OH measurements indicate a kinetic temperature of ≈ 450 K in both helium and argon lamps at 1.5 torr and 20 watts; the normal operating conditions of the lamps.

This temperature is somewhat lower than we had expected based upon results of other investigators.[6,12] We have noticed, however, that lamp kinetic temperatures appear to vary with lamp diameter, probably due to improved heat transfer to the lamp walls in smaller lamps. In the present studies the lamp walls were thicker than is normal for 12 mm tubing. Thus the inside diameter of these lamps was smaller than is normal for 12 mm lamps.

## 3.2 Absorption Measurements

The absorption of various number densities of $N(^2D)$ was determined for a helium lamp operating at normal conditions and a number of argon lamps under a variety of lamp conditions. The experimental arrangement is described in detail in Sec. 3 of Appendix A. The $N(^2D)$ number density was varied by reaction with $CO_2$:

$$N(^2D) + CO_2 \rightarrow CO + NO \qquad (4)$$

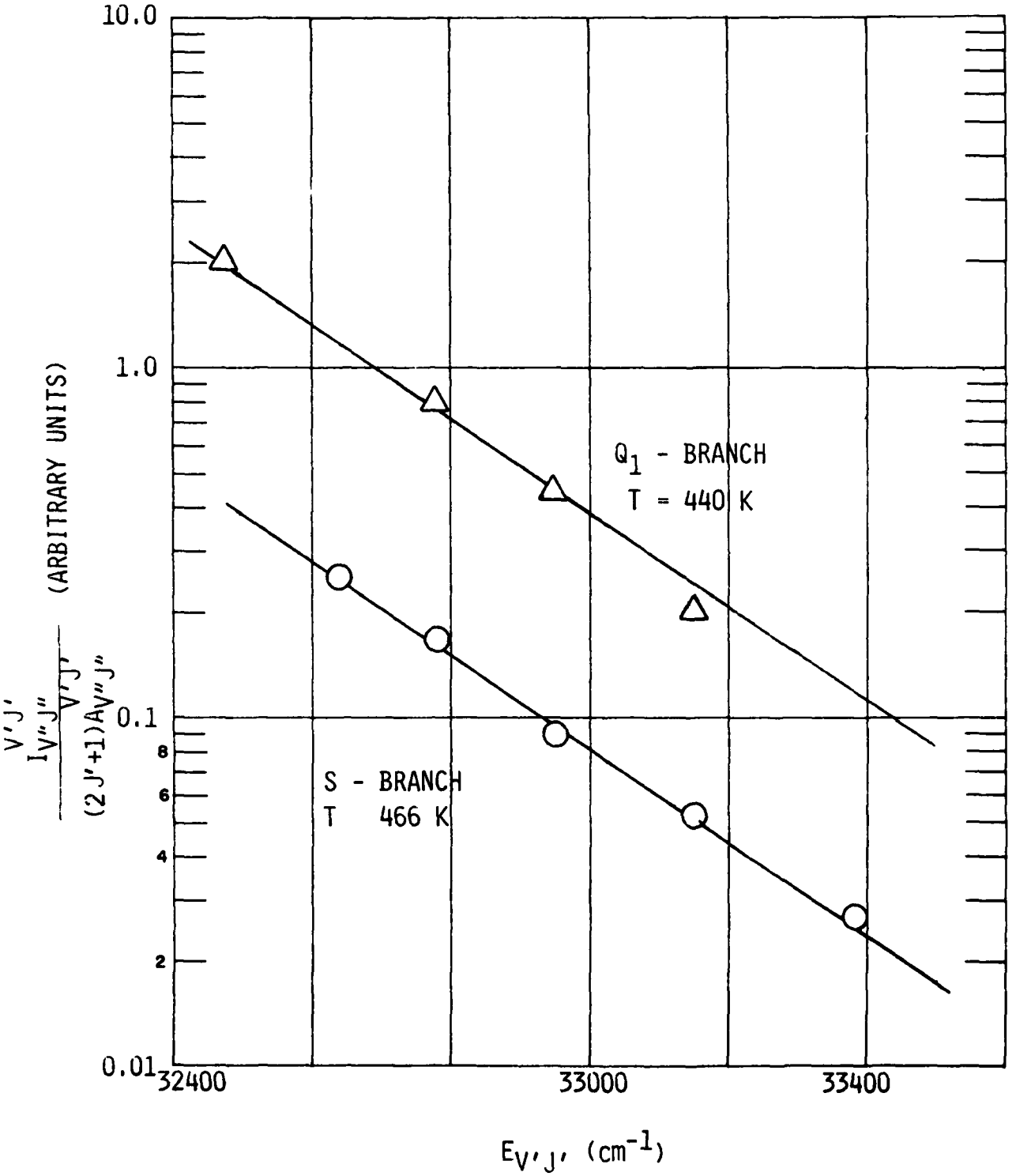


Fig. 3 Maxwell-Boltzmann rotational plot for a 30 watt lamp in 2 torr of helium and 7 mtorr $H_2O$.

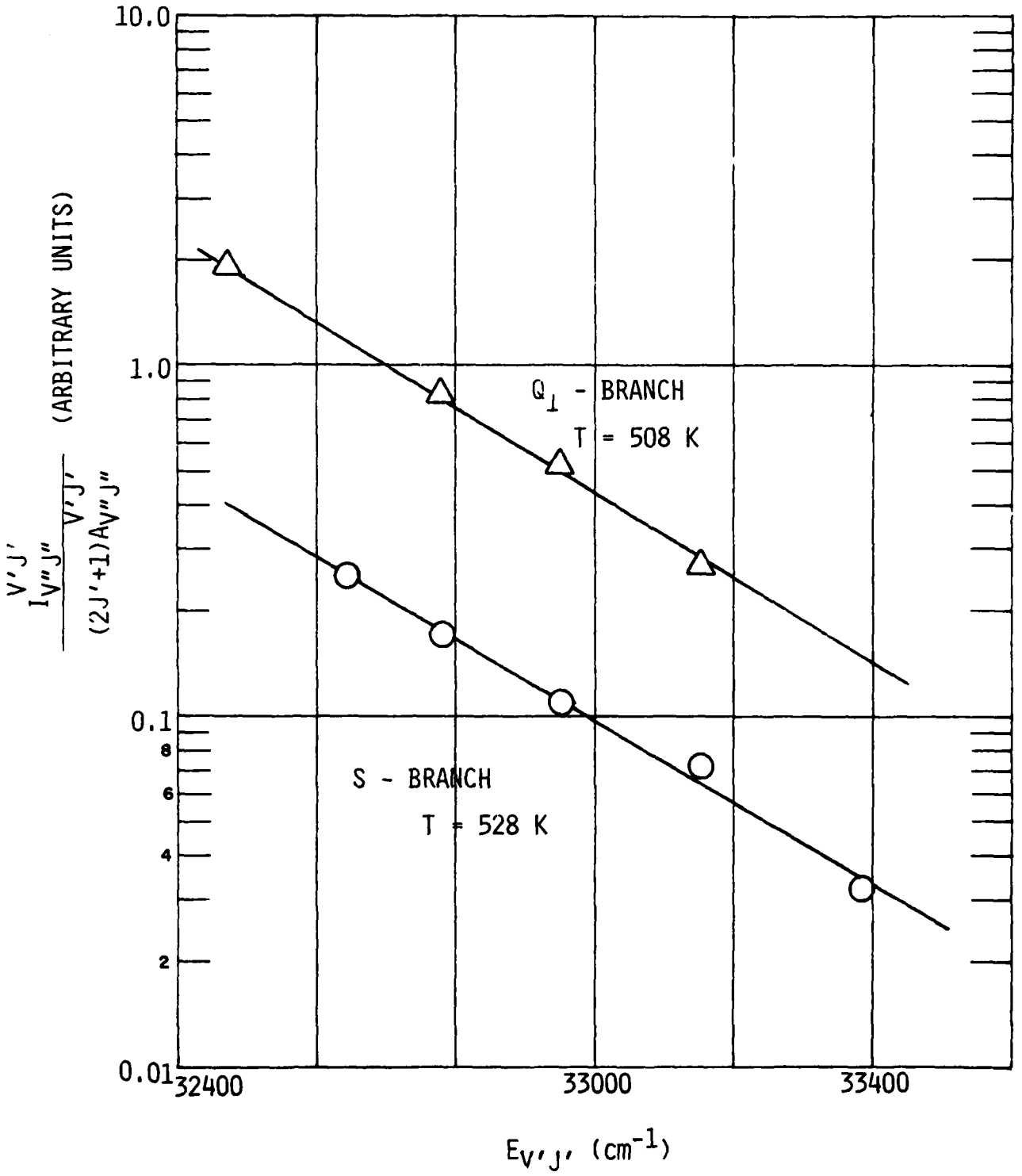


Fig. 4 Maxwell-Boltzmann rotational plot for a 50 watt lamp in 2 torr Ar and 7 mtorr $H_2O$.

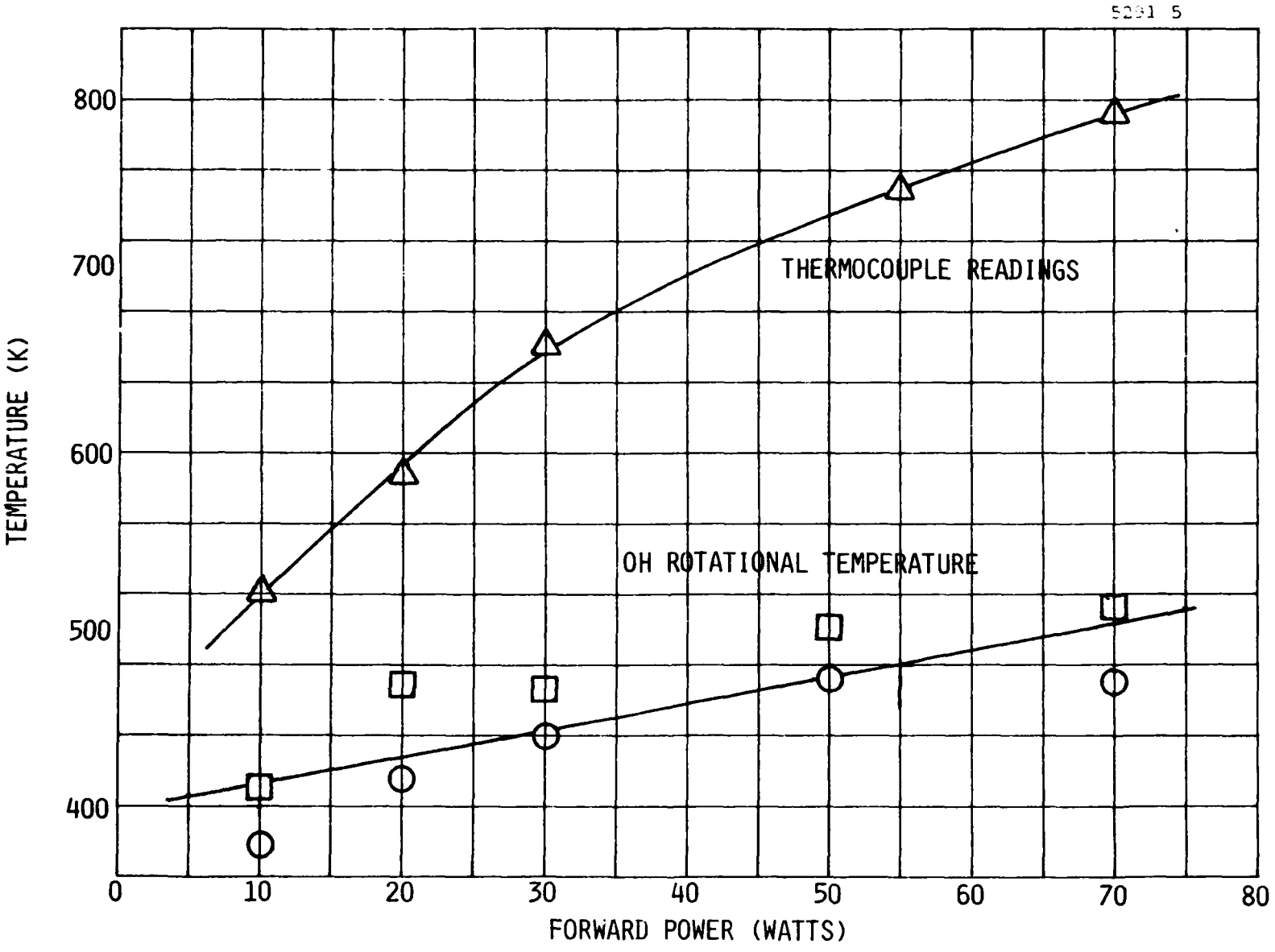


Fig. 5 The temperature of a 2 torr helium/water lamp ($X_{H_2O} \approx 0.003$) as a function of discharge power (O $Q_1$- branch; □ S-branch).

5291--6

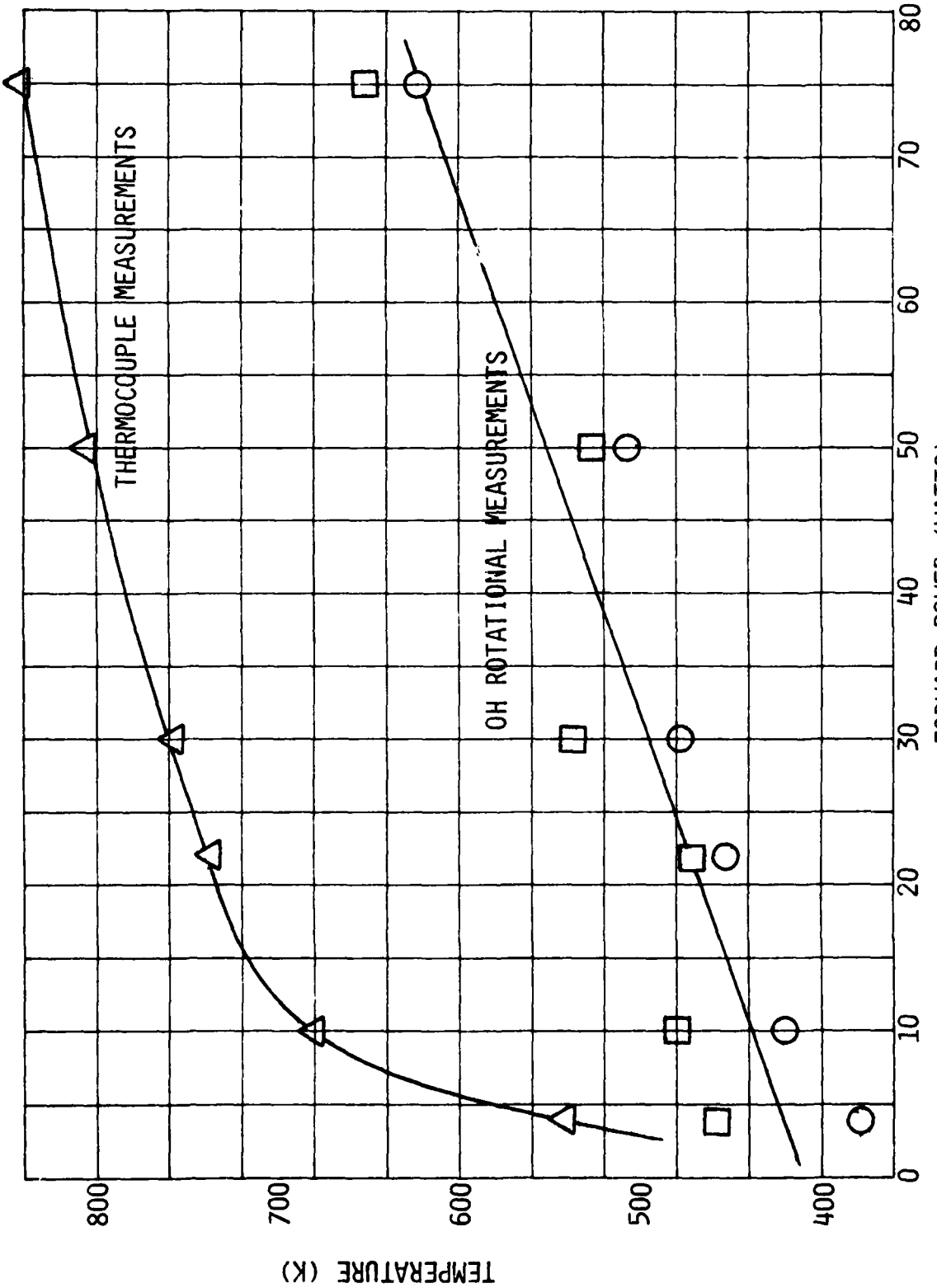


Fig. 6 The temperature in a 2 torr argon/water lamp ($X_{H_2O} \approx 0.003$) as a function of discharge power. (O $Q_1$-branch; □ S-branch).

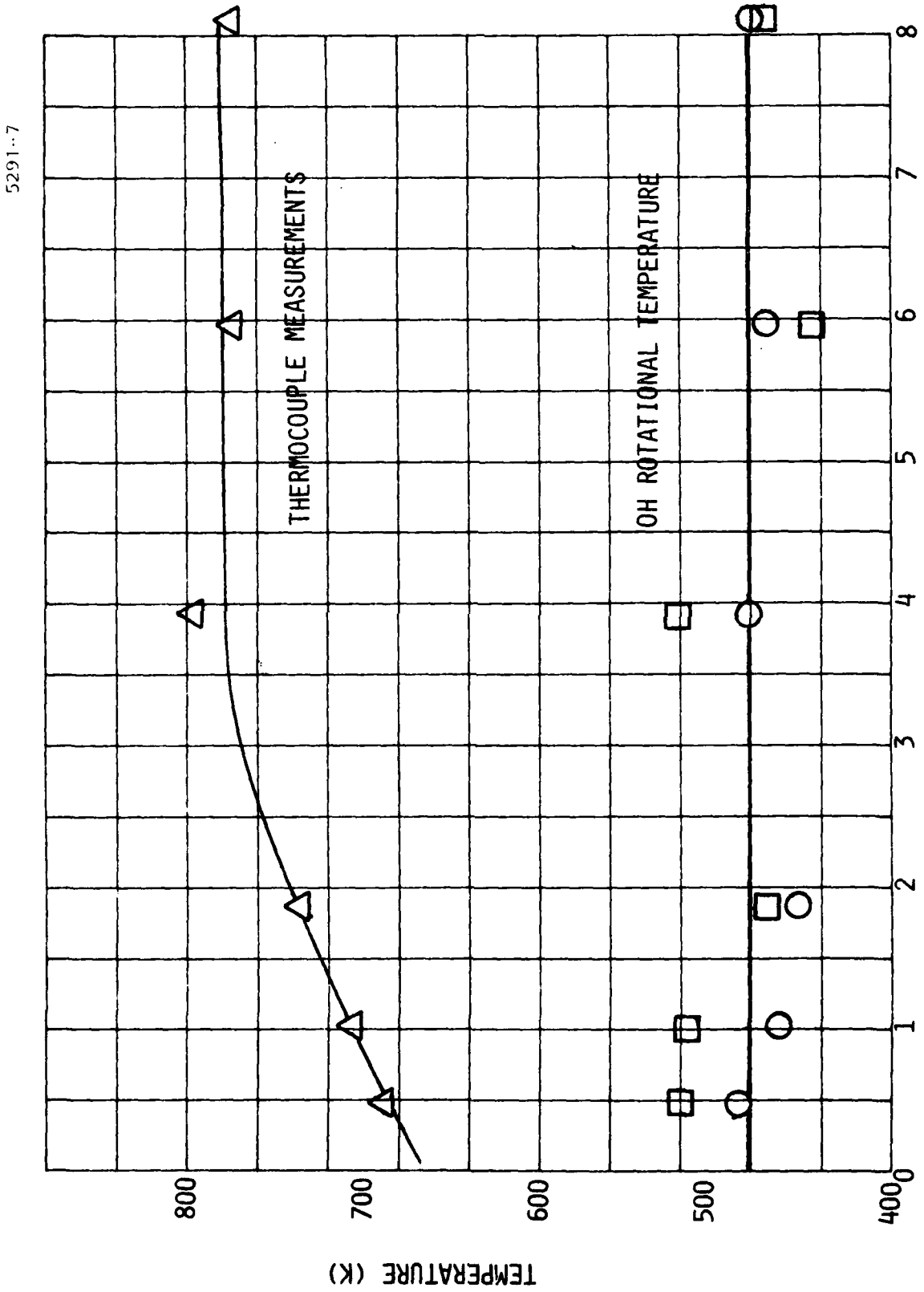


Fig. 7 The temperature in a 20 watt argon/water ($X_{H_2O} \approx 0.003$) lamp as a function of lamp pressure. (O $Q_1$-branch; □ S-branch).

A correlation of $\ell n\ 1/(1-A)$, where A was the absorption for $N(^2D)$ using a helium lamp, versus $[CO_2]$ placed the $N(^2D)$ number density upon a relative scale for further lamp measurements. Complete integration of the absorption equations showed that the Beer's-Law analogue, $\ell n\ 1/(1-A)$, was linear in $[N(^2D)]$ to within 5% over the range of absorptions measured ($A < 0.26$). Figure 8 shows the correlation plot of $[N^*]_{rel}$ versus $[CO_2]$.

Over the range of $[N(^2D)]$ covered in this study, the curves-of-growth of A versus $[N^*]_{rel}$ could be fit to a two parameter polynomial:

$$A = \frac{[N^*]_{rel}}{(1 + \alpha^2)^{1/2}} - \gamma[N^*]^2_{rel} \qquad (5)$$

We analyzed the curves-of-growth with a linear least-squares fit to the equation

$$\frac{A}{[N^*]_{rel}} = \beta - \gamma[N^*]_{rel} \qquad (6)$$

Realistic fits obtained only when the experimental data were properly weighted. Figures 9 and 10 show several representative curves-of-growth along with the best-fit lines from Eq. (6).

The effective Doppler temperature in the argon lamps can be determined if an effective temperature is assumed in the helium-lamp measurements from the ratio of the linear terms in Eq. (5) from the two types of lamps. Thus

$$T_{Ar} = 300\alpha^2_{Ar} = \left(\frac{\beta_{He}}{\beta_{Ar}}\right)^2 (1 + \alpha^2_{He}) - 1 \qquad (7)$$

The ratio $\beta_{He}/\beta_{Ar}$ is 2.2, which implies an effective emission line temperature of 3650 K assuming a temperature in the helium lamp of 450 K.

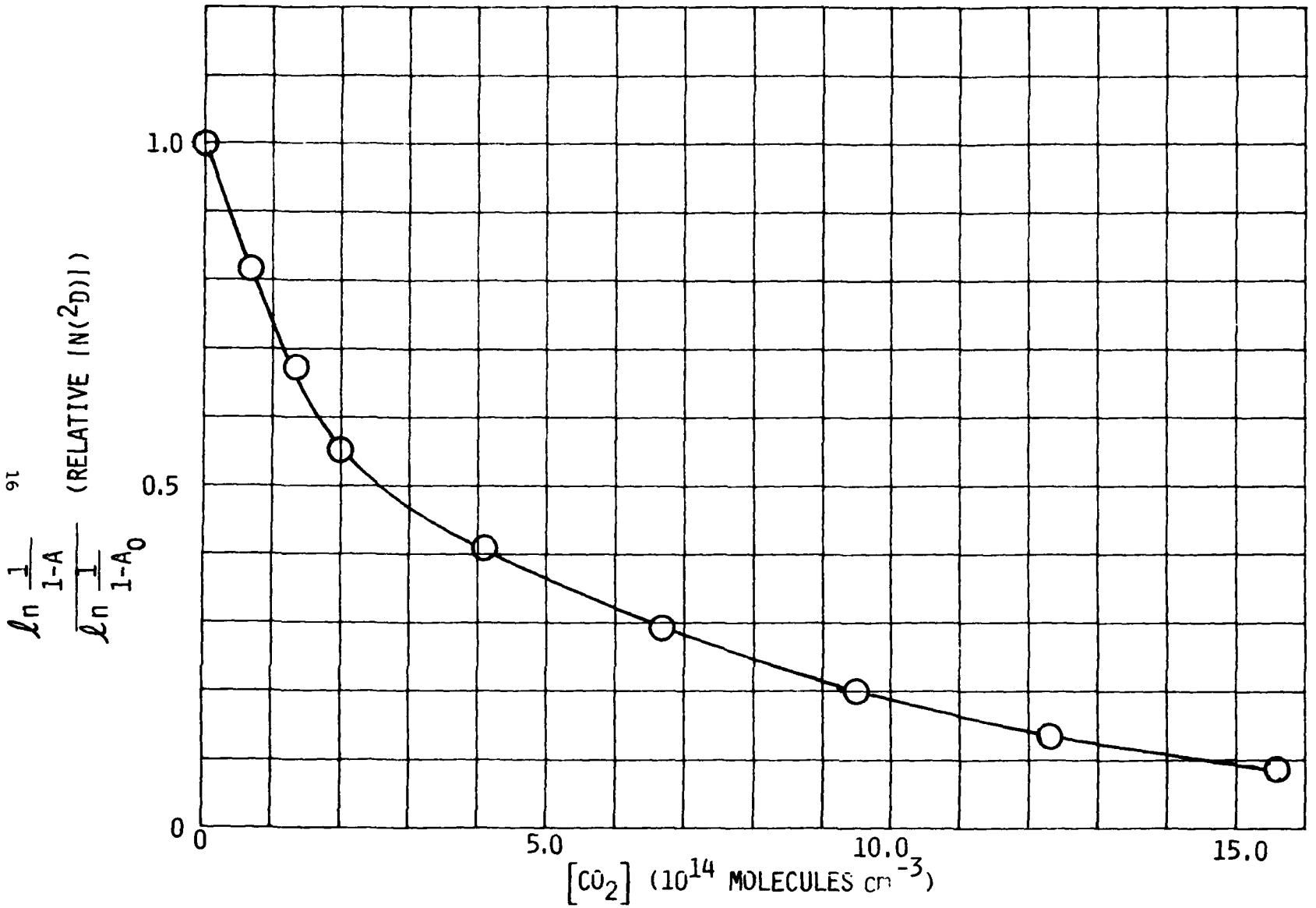


Fig. 8 Correlation between relative N($^2$D) number density and amount of $CO_2$ titrant in reactor.

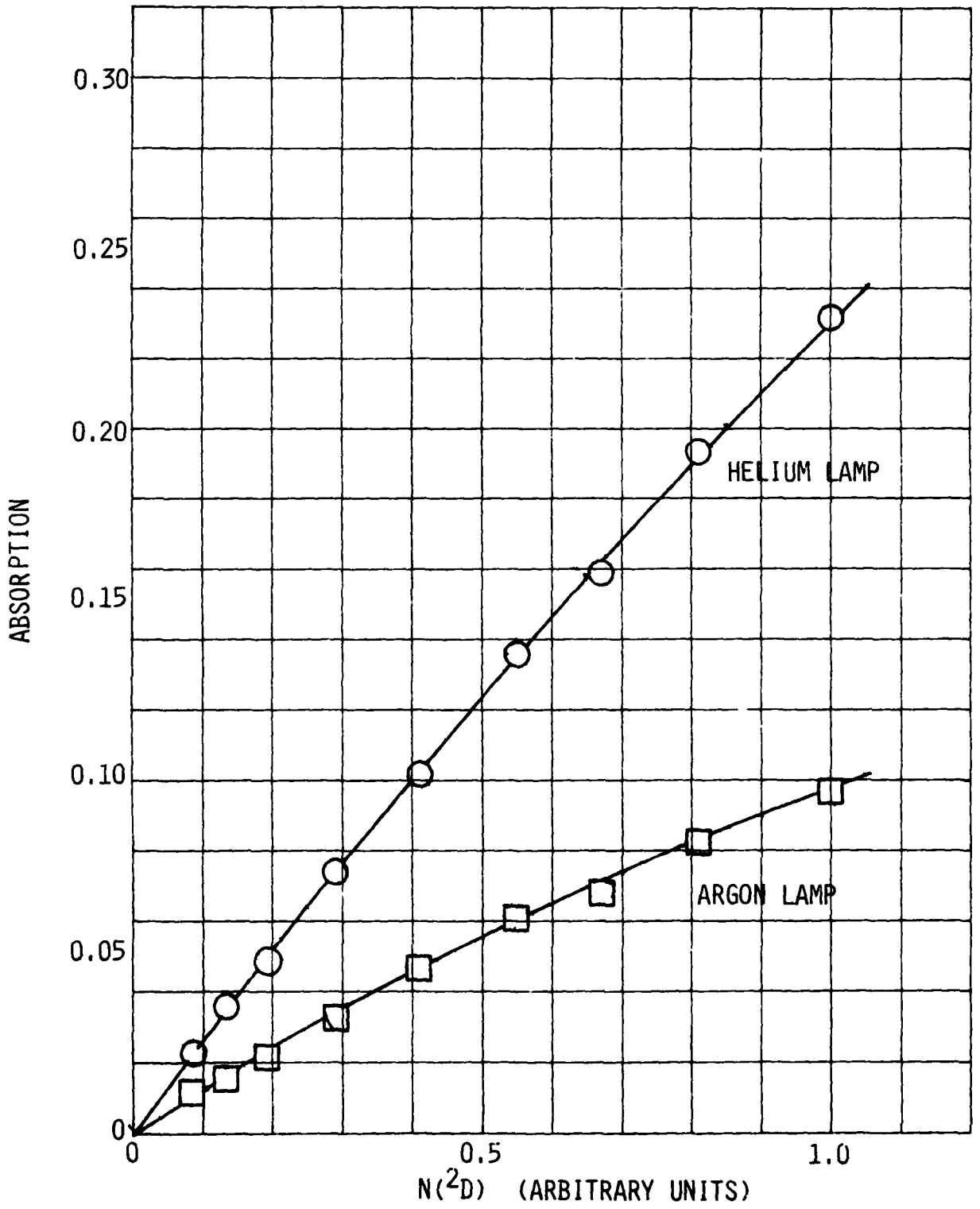


Fig. 9 Absorption of various $N(^2D)$ number densities from 20 watt argon and helium lamps at 1.5 torr.

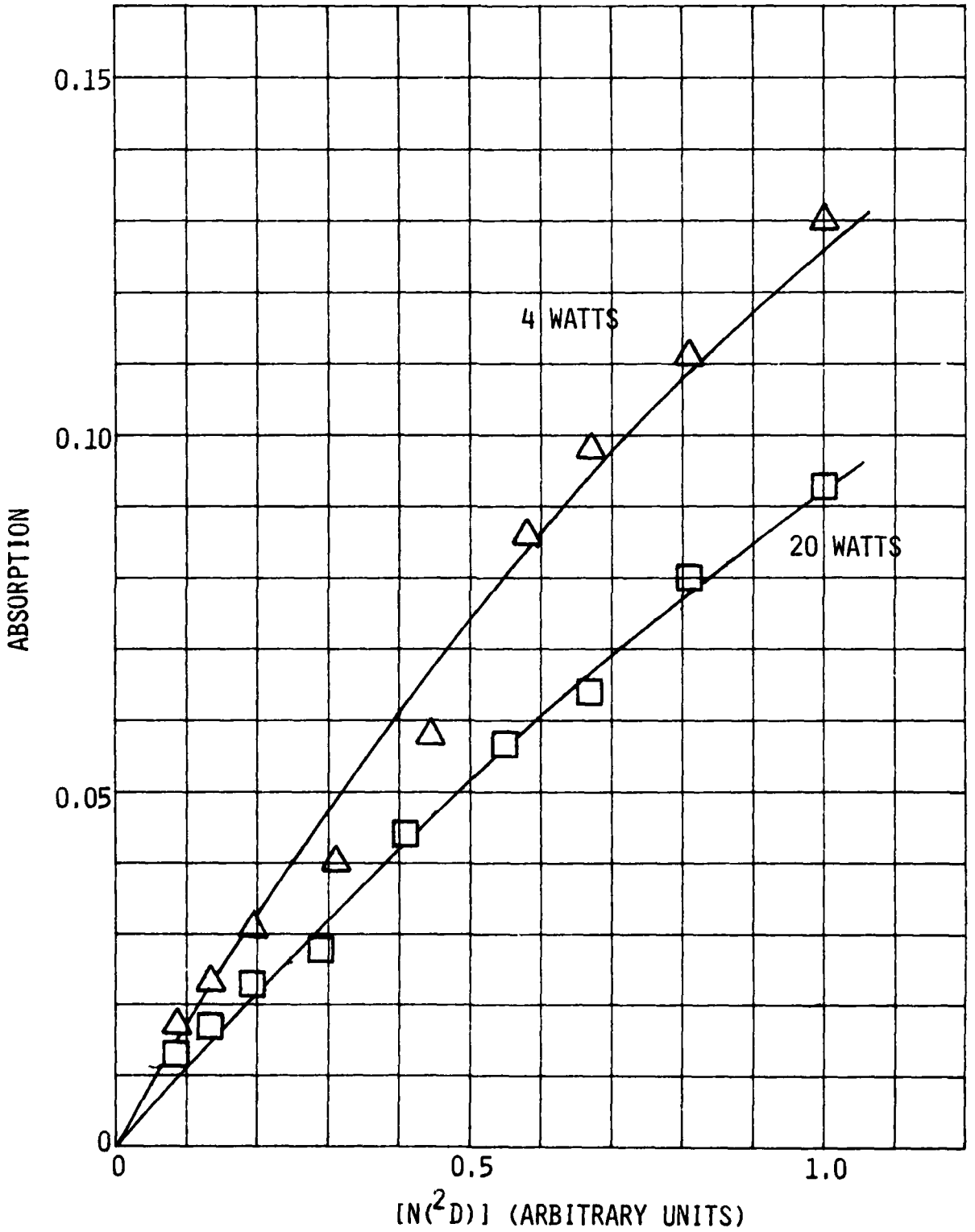


Fig. 10 Absorption of $N(^2D)$ from argon lamps at 1.5 torr.

Figure 11 shows how the ratio of $N(^2D)$ absorption for argon lamps at several pressures to the absorption from a 1.5 torr argon lamp varies with pressure. The data indicate a slight increase in absorption at higher pressures which results from collisional narrowing of the lineshape function by collisions which reduce the excess translational energy of the excited atoms prior to emission.

Figure 12 shows how the argon lamp absorption varies with forward power compared to a 20 watt argon lamp. Only at extreme high and low powers are the differences significant. The low power point probably indicates a larger importance of electron impact excitation relative to metastable excitation compared to the standard case. Further investigation would be interesting.

We investigated the possibility of modifying the excitation mechanisms in the argon lamp to enhance excitation by electrons relative to that by metastable argon. Xenon in varying number densities was added to the argon flow. Xenon is known to be a rapid quencher of metastable argon with a quenching rate constant at $1.8 \times 10^{-10}$ $cm^3$ $molecule^{-1}$ $s^{-1}$.[13] The long-lived metastable energy levels of xenon which are produced by a radiative cascade process in the transfer of energy between $Ar(^3P_2)$ and Xe[14] are too low in energy to excite the 3s $^2P$ level of atomic nitrogen in an energy-transfer reaction. The results of the experiments showed no change in absorption at 149.3 nm by the metastable $N(^2D)$ even at xenon number densities as high as $3 \times 10^{15}$ atoms $cm^{-3}$ (see Fig. 13). We had anticipated that the absorption at 149.3 nm for a constant $[N(^2D)]$ would increase as the electron excitation branch became a more significant fraction of the total N (3s $^2P$) excitation. The intensity of the 149.3 nm line was reduced by a factor of five at the maximum xenon number density, indicating that some quenching of the metastable argon by the xenon was taking place, but clearly that amount of quenching was not sufficient to alter the primary excitation mechanism in the lamp.

### 3.3 Summary of Calibration Experiments

The lamp calibration experiments show clearly that the major mechanism for excitation of the 149.3 and 174.3 nm lines in an argon lamp is the transfer of electronic energy from metastable argon atoms to ground-state nitrogen

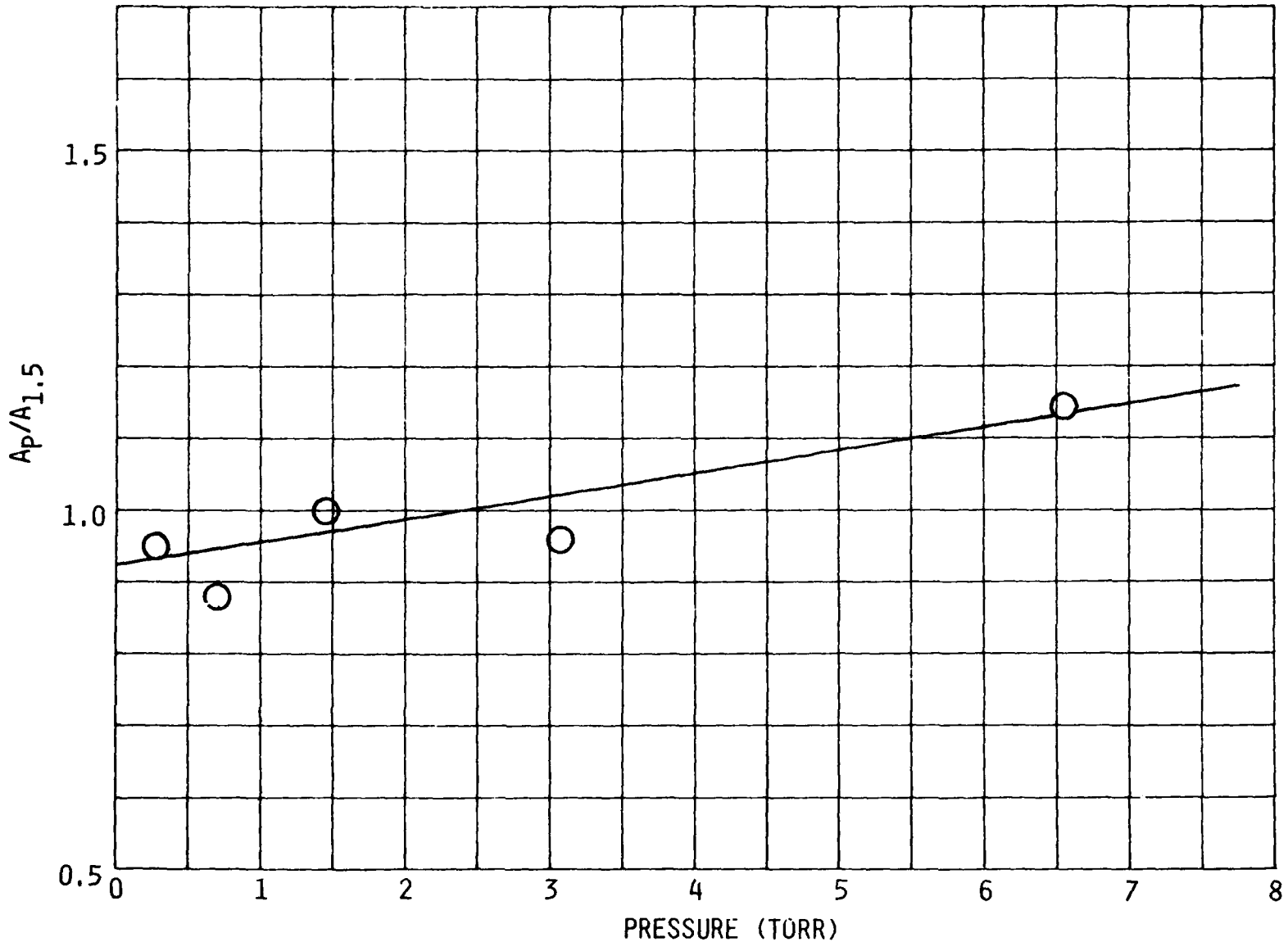


Fig. 11 Variation in the ratio of absorbance of $N(^2D)$ from a 2.0 watt argon lamp to that from a 1½ torr lamp as a function of pressure.

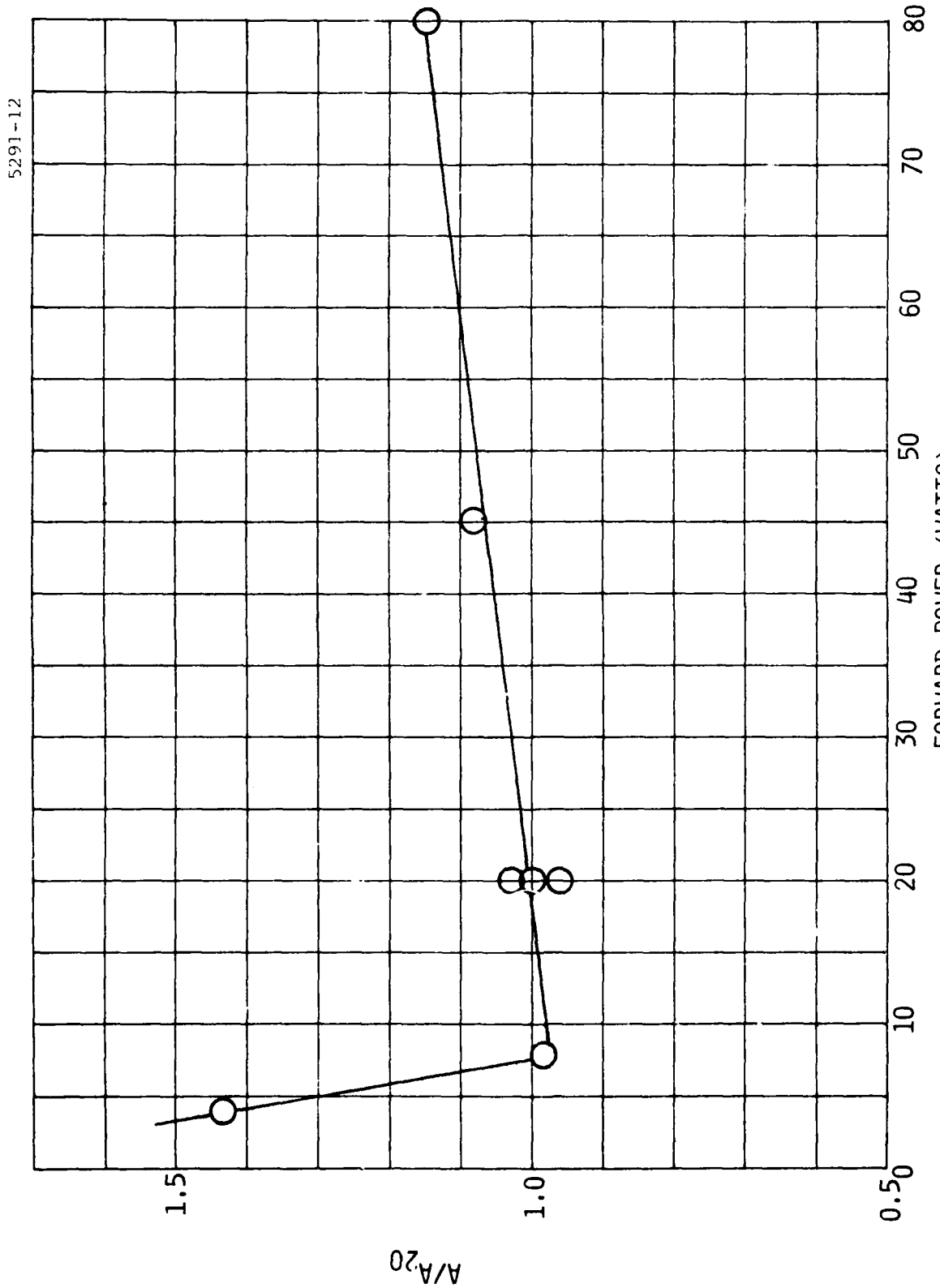


Fig. 12 Variation in the ratio of $N(^2D)$ absorbance from a 1.5 torr argon lamp to that of a 20 watt lamp as a function of discharge power.

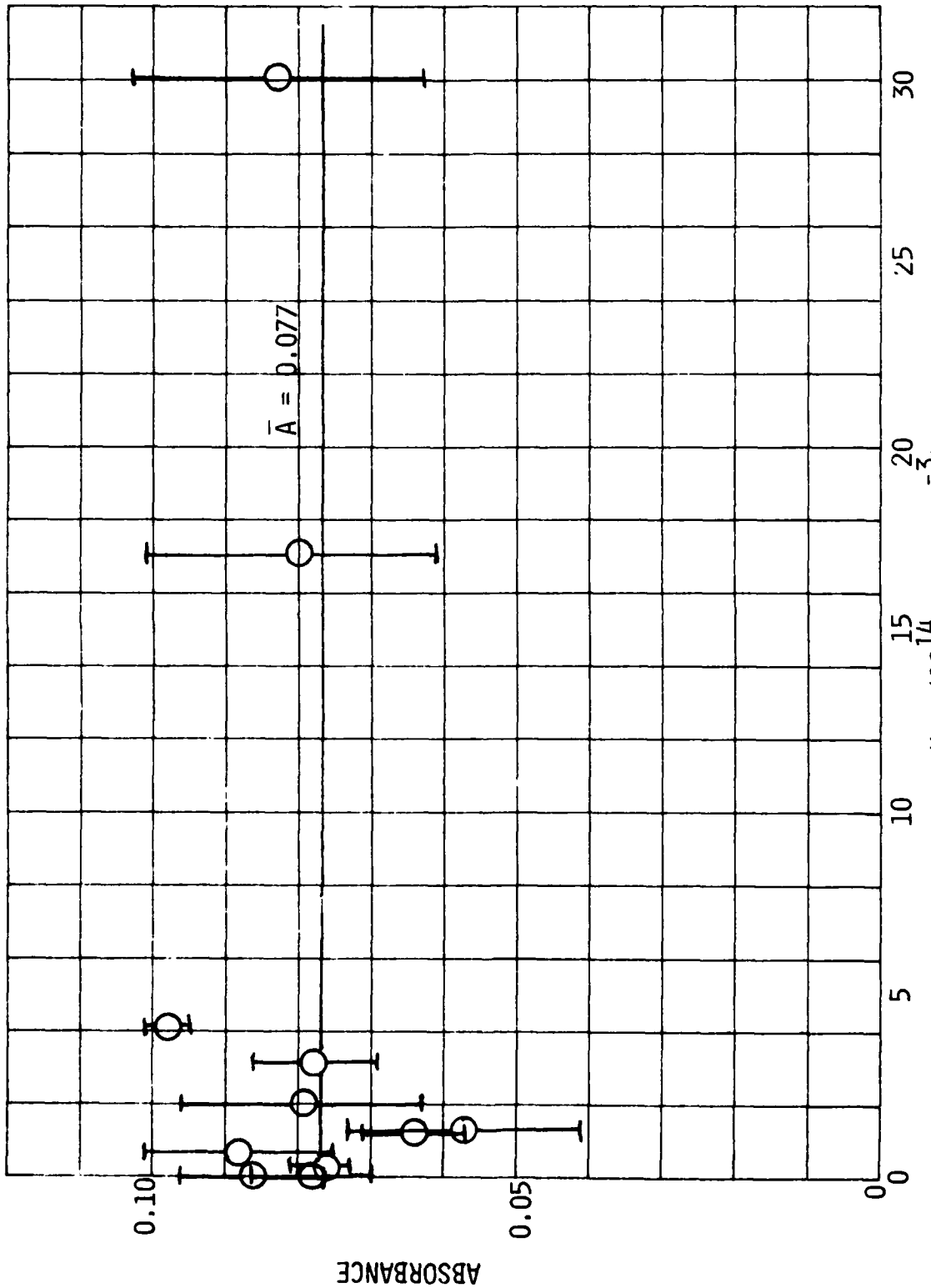


Fig. 13 $N(^2D)$ absorbance from ' torr argon lamp as a function of added xenon.

atoms. The electronically excited nitrogen atoms are also excited translationally, and this translational excitation results in broadened emission profiles at 149.3 and 174.3 nm with an effective temperature of 4000 K. The effective translational temperature of the emitting atoms is not very sensitive to changes in lamp pressure or power.

## 4. SUMMARY

VUV resonance absorption measurements at 149.3 nm are a sensitive diagnostic for metastable nitrogen atoms ($N(^2D)$). Low power, low pressure rare-gas discharge lamps containing traces of molecular nitrogen are good sources of the 149.3 nm radiation.

The Doppler broadening of the 149.3 nm line in an argon lamp is much greater than that in a helium lamp because, in an argon lamp, the 149.3 nm radiation is excited in a highly exoergic rare-gas metastable energy-transfer reaction as opposed to electron-impact excitation in the helium lamp. This increased Doppler broadening in the argon lamp means that argon lamps make less sensitive diagnostics than helium lamps. However, the Doppler broadening in the argon lamp is likely to be insensitive to variations in lamp temperature, unlike the helium-lamp case, so that argon-lamp calibrations carried out at room temperature should be reasonably accurate in the 80 K environment of COCHISE. Our calculations indicated that an absorption diagnostic based upon an argon lamp should have a sensitivity of $1 \times 10^9$ atoms $cm^{-3}$ for $N(^2D)$ in COCHISE which should be more than adequate for the proposed $N(^2D)$ measurements. We therefore built a 149.3 nm absorption for $N(^2D)$ atoms in COCHISE using an argon lamp as the line source. The component parts of the diagnostic, lamp, reflector, detector, and all necessary electrical and plumbing services were delivered to the Air Force Geophysics Laboratory in September, 1981.

## REFERENCES


1. J. P. Kennealy, F. P. DelGreco, G. E. Caledonia and W. T. Rawlins, "COCHISE: Laboratory Spectroscopic Studies of Atmospheric Phenomena with High-Sensitivity Cryogenic Instrumentation," Proc. Soc. Photo-Opt. Instrumentation Eng. (G. A. Vanasse, ed.), 191, 151 (1979).

2. L. G. Piper and W. T. Rawlins, "Development of COCHISE UV Absorption System," PSI TR-239, TR-251 and TR-264 under Air Force Contract No. F19628-80-C-0174 (1980, 81).

3. W. T. Rawlins and L. G. Piper, "Effects of Excitation Mechanism on Linewidth Parameters of Conventional VUV Discharge Line Sources," Proc. Soc. Photo-Opt. Inst. Eng. 279, 58 (1981).

4. L. G. Piper and W. T. Rawlins, "Effects of Excitation Mechanism on Linewidth Parameters of Conventional VUV Discharge Line Sources," 34th Annual Gaseous Electronics Conference, Boston, 20-23 October 1981. Bull. Am. Phys. Soc. xx, xxx (1981).

5. J. P. Kennealy, F. P. DelGreco, G. E. Caledonia, and B. D. Green, "Nitric Oxide Chemi-excitation Occurring in the Reaction Between Metastable Nitrogen Atoms and Oxygen Molecules," J. Chem. Phys. 69, 1574 (1978).

6. C. L. Lin and F. Kaufman, "Reactions of Metastable Nitrogen Atoms," J. Chem. Phys. 55, 3760 (1971).

7. G. E. Caledonia, B. D. Green, G. A. Simons, J. P. Kennealy, F. X. Robert, A. Corman and F. P. DelGreco, "COCHISE Studies I: Fluid Dynamic and Infrared Spectral Analysis," Air Force Geophysics Laboratory TR-77-0281, Environmental Research Paper #619, 9 December 1977.

8. B. K. Flint, "Special Application Coatings for the Vacuum Ultraviolet," Proc. Soc. Photo-Opt. Instrumentation Eng. (G. A. Vanasse, ed.), 140, Paper 14 (1978).

9. M. Iannuzzi and F. Kaufman, private communication, 1979.

10. W. R. Hunter and S. A. Malo, "The Temperature Dependence of the Short Wavelength Transmittance Limit of Vacuum Ultraviolet Window Materials - I. Experiment," J. Phys. Chem. Solids 30, 2739 (1969).

11. I. L. Chidsey and D. R. Crosley, J. Quant. Spectrosc. Radiat. Transfer 23, 187 (1980).

12. M. A. A. Clyne and L. G. Piper, JCS Faraday II, 72, 2178 (1976).

13. L. G. Piper, J. E. Velazco, and D. W. Setser, "Quenching Cross Sections for Electronic Energy Transfer Reactions Between Metastable Argon Atoms and Noble Gases and Small Molecules," J. Chem. Phys. 59, 3323 (1973).

14. D. L. King, L. G. Piper, and D. W. Setser, "Electronic Energy Transfer from Metastable Argon (4s $^3P_{2,0}$) to Xenon, Oxygen and Chlorine Atoms," JSC Faraday II 73, 177 (1977).

APPENDIX A

# EFFECTS OF EXCITATION MECHANISM ON LINEWIDTH PARAMETERS OF CONVENTIONAL VUV DISCHARGE LINE SOURCES

by

Wilson T. Rawlins and Lawrence G. Piper

PHYSICAL SCIENCES INC.
30 Commerce Way
Woburn, MA 01801

## ABSTRACT

Conventional vacuum ultraviolet line sources often consist of electrodeless rf or microwave discharges of flowing or sealed inert gases at 1-10 torr. The inert buffer, typically helium or argon, is seeded with traces of parent species of the desired transitions (e.g., $O_2$ or $N_2$ for OI or NI transitions, respectively). The sensitivity of resonance sources as absorption or fluorescence diagnostics depends critically upon the effective line width of the source resonance radiation. This property is determined primarily by source self-absorption, and by Doppler broadening of the source radiation, which is itself a function of the translational-energy distribution of the radiating species. Self-absorption is easily minimized or characterized experimentally. However, Doppler broadening is a complex function of the lamp excitation processes and should be characterized for each type of resonance lamp. The major competing excitation mechanisms for transitions such OI(130 nm) or NI(120 nm, 149 nm, 175 nm) in such line sources are electron impact processes, where the excess kinetic energy of the collision is retained with the electrons, and energy transfer or dissociative excitation by rare gas metastables ($Ar(^3P_{2,0})$ at 11.5 eV or $He(2^{3,1}S)$ at $\approx$ 20 eV), where a significant fraction of the energy defect may appear as excess translational energy in the radiating species. The kinetics of these processes as they relate to various VUV atomic line sources are reviewed. In addition, preliminary experimental data from absorption measurements on atomic nitrogen metastables, $N(^2D)$ and $N(^2P)$, produced in a discharge-flow apparatus, are presented which show markedly different

behavior between microwave-excited $He/N_2$ and $Ar/N_2$ lamps. The implications of these effects for design application of resonance absorption/fluorescence diagnostics are illustrated.

# 1. INTRODUCTION

Atomic line sources in the vacuum ultraviolet are used extensively for resonance absorption and fluorescence measurements both in the laboratory and in the upper atmosphere. In the laboratory, these techniques have been used by many investigators to study reactions of O, Cl, H, $N(^4S)$, $N(^2D)$, $N(^2P)$, and many others.[1] These studies have employed a variety of resonance line sources, but the majority have used sources which are excited by microwave discharge of trace impurities in a few torr of flowing helium or argon.[2] In upper atmospheric experiments, a variety of microwave and rf-excited discharges of static helium (with controlled trace impurities) have been used in rocket,[3] balloon,[4] and spacecraft[5] measurements of species such as O, $N(^4S)$, Cl, and OH in the stratosphere, mesosphere, and thermosphere.

In all of these types of applications, it is important, from the standpoint of experiment design, measurement sensitivity, and absolute calibration, to be able to model analytically the absorption process in terms of physically realistic mechanisms. The fractional absorption over a line is determined by the degree of overlap between emitter and absorber lineshape functions, as shown in Fig. 1. These functions must be described in terms of the various line broadening mechanisms. For the great majority of laboratory and atmospheric measurements, the absorber lineshape is governed by Doppler broadening at the ambient temperature (usually a Gaussian line profile), and in some cases by collisional (pressure) broadening (Lorentzian line profile). Both of these sources are relatively easy to characterize experimentally. The major unknown quantity in absorption measurements then is the effective line width of the resonance emission from the discharge lamp. Typical VUV linewidths are too small to be resolved by conventional spectrometers; thus they must be determined in carefully defined calibration experiments.

The effective emission line width is affected primarily by self-absorption in the source and by excitation processes in the discharge plasma. Self-absorption can be minimized experimentally or characterized analytically in a straightforward manner (see below). However, the excitation processes in the discharge can have marked effects upon the emission line width characteristics and upon their variation with lamp temperature, pressure, and mode

of excitation. This has been found, for example, in the case of atomic oxygen (OI) resonance lamps operating on the 130 nm resonance triplet[6] where the emission line widths in helium-filled microwave and radio-frequency discharge lamps have been shown to vary strongly with pressure and applied power. It is imperative therefore to characterize experimentally each type of line source to be used.

For the case of OI line sources, mechanisms for the excitation of the resonance radiation in He and Ar are well-studied[6-8]; the major pathways are via direct electron impact processes, dissociative excitation of $O_2$ by He metastables,[7] and energy transfer to O by Ar metastables.[8] The rare gas metastable reactions often dominate the electron impact route and impart substantial excess kinetic energy to the radiating atoms, thus broadening the net emission line. In this paper we review the available data on the energy-transfer reactions which provide important excitation pathways for helium- and argon-filled lamps emitting the OI (130 nm) and NI(120, 149, and 174 nm) multiplets, and show how these data can be used to explain adequately the observed characteristics of OI and NI resonance lamps. We also present preliminary results from a laboratory program to characterize experimentally the NI resonance multiplets at 149 and 174 nm which are diagnostic of $N(2p^4$ and $N(2p^4\,^2P)$, respectively. The motivation of this study is to develop VUV resonance absorption capability for the cryogenic infrared facility COCHISE,[9] where in situ calibrations are not possible and the line width characteristics of the various lamps must be extrapolated reliably from room-temperature experiments to cryogenic (~ 100 K) conditions. In the following sections, the mathematics of the absorption model are briefly reviewed, experimental methods for lamp characterization and calibration are described, and the behavior of OI and NI resonance lamps is discussed in terms of the detailed kinetics of the various mechanisms in the lamp.

## 2. THEORY OF RESONANCE ABSORPTION

Atomic number densities can be determined by measuring the fractional absorption of the resonance lines emitted by a lamp. This fractional absorption is then related to the absorption coefficient of the resonance transition, $k_\nu$ (which is itself a function of frequency, $\nu$, as well as number density of absorbers, N), through Eq. (1):[10]

$$A = \frac{I_o - I_{trans}}{I_o} = \frac{\int_{-\infty}^{\infty} I(\nu) \left(1 - e^{-k_\nu \ell}\right) d\nu}{\int_{-\infty}^{\infty} I(\nu)\, d\nu} \qquad (1)$$

where $I(\nu)$ is the frequency-dependent emission intensity and $\ell$ is the path length over which the absorption measurements are being made. If the absorption line width is determined primarily by Doppler broadening with a Maxwell-Boltzmann translational energy distribution, the absorption coefficient is given by

$$k_\nu = k_o\, e^{-\omega^2} \qquad (2)$$

where $k_o$ is the absorption coefficient at line center, and the reduced frequency $\omega$ is given by

$$\omega = \frac{2(\nu - \nu_o)}{\Delta\nu_D} \sqrt{\ell n 2} \quad , \qquad (3)$$

$\nu_o$ is the frequency of the line center and $\Delta\nu_D$ is the full width at half maximum of the absorption line as determined by Doppler broadening. In some applications, the pressure is sufficiently high that collisional broadening also plays a role, and $k_\nu$ must be expressed in terms of the so-called Voigt profile which combines the effects of Doppler and collisional

broadening.[10] Methods of accounting for non-Doppler broadening processes such as collisional, electron-induced, and natural (uncertainty) broadening of resonance lines have been reviewed by Clyne and Piper.[11] The treatment of broadening resulting from nuclear or isotopic hyperfine splitting is discussed by Tellinghuisen and Clyne[12] and Clyne and Smith.[13] None of these contributions are applicable for the range of pressures, electron densities, or species encountered in the present study.

The absorption coefficient at line center, $k_o$, is a function of the number density of absorbers, N, and their oscillator strength, f,

$$k_o = \frac{2}{\Delta\nu_D}\left(\frac{\ell n\ 2}{\pi}\right)^{1/2}\frac{\pi e^2}{m_e c}\,Nf \qquad (4)$$

where $m_e$ and e are the electron mass and charge (esu), respectively, and c is the speed of light. The Doppler full width at half maximum, $\Delta\nu_D$, is

$$\Delta\nu_D\ (s^{-1}) = \frac{2}{\lambda_o}\left(\frac{2RT\ell n2}{M}\right)^{1/2} \qquad (5)$$

where R is the gas constant, T the temperature, M the molecular weight and $\lambda_o$ the central wavelength of the transition.

In most cases the emission line shape can also be modeled in terms of Doppler broadening with a Maxwell-Boltzmann temperature distribution, but with a different effective temperature than that of the absorption line shape. Then the effective emission-line width differs from the absorber Doppler line width by the parameter $\alpha$, which is the square root of the ratio of the effective temperature of the emission source to the temperature of the absorbers. Thus,

$$I(\nu) = I_o\, e^{-(\omega/\alpha)^2} \qquad (6)$$

and the integral expression for A becomes

$$A = \frac{I_o - I_{trans}}{I_o} = \frac{\int_{-\infty}^{\infty} \left(1 - e^{-k_o \ell e^{-\omega^2}}\right) e^{-(\omega/\alpha)^2} \, d\omega}{\int_{-\infty}^{\infty} e^{-(\omega/\alpha)^2} \, d\omega} \quad . \tag{7}$$

The actual emission line shape may differ from the Gaussian form of Eq. (6) due to self-absorption (which preferentially affects the center of the line) or monoenergetic excitation processes (e.g., energy transfer from metastable Ar). Mathematical treatments of these effects have been given by Kaufman and co-workers[6,14] and by Clyne and co-workers.[12,13,15] The self-absorption model of Rawlins and Kaufman[6] gives an excellent match to OI absorption data over a wide range of lamp optical thickness. Self-absorption is not a factor in the experiments we will describe and will not be considered further; however, its inclusion in some applications (such as that of Ref. 5) can be vitally important. Monoenergetic effects are often collisionally moderated in steady-state line sources. In any case, since only the integral over the line is observed, such profiles often, but not always,[13] can be approximated by the Doppler formulae with little loss of generality.[6]

Equation (7) can be integrated in a straightforward manner by the method of Gaussian quadrature. However, for the purpose of the present discussion, the following analytic expression for A is useful:

$$A = \sum_{n=1}^{\infty} (-1)^{n-1} \frac{(k_o \ell)^n}{n! \, (1+n\alpha^2)^{1/2}} \quad . \tag{8}$$

In the limit of small optical depth, $k_o \ell$, only the first term is significant, and Eq. (8) reduces to

$$A \simeq \frac{k_o \ell}{(1+\alpha^2)^{1/2}} \tag{9}$$

The above expressions hold only in the case of a single line. However, the 149 and 174 nm transitions consist of multiplets which are difficult to resolve fully. For the case of unresolved multiplets (line separation << instrument resolution), an expression similar to Eq. (7) holds:

$$A = \frac{\sum_i C_i \int_{-\infty}^{\infty} \left(1 - e^{-k_{oi} \ell e^{-\omega_i^2}}\right) e^{-(\omega_i/\alpha)^2} \, d\omega}{\sum_i C_i \int_{-\infty}^{\infty} e^{-(\omega_i/\alpha)^2} \, d\omega} \qquad (10)$$

where the $C_i$ represent the relative intensities of the components of the multiplet. The spectroscopic properties of the $N(^2D)$ and $N(^2P)$ resonance multiplets are given in Table I.

## 3. EXPERIMENTAL METHODS

The resonance lamp characterization measurements are carried out on a discharge-flow apparatus, with the same basic approach as that of Ref. 6: known concentrations of the absorbing species are produced in the flow reactor, and the resonance absorption of the line radiation from a given discharge lamp is measured as a function of absorber concentration. The apparatus is essentially the same as that described elsewhere[16] except for minor modifications to provide VUV resonance absorption/fluorescence capability. The basic apparatus, shown in Fig. 2, consists of a two-inch (i.d.) discharge-flow system which is pumped by a Leybold-Heraeus Roots blower/forepump combination capable of producing linear flow velocities up to $8 \times 10^3$ cm $s^{-1}$ at 1 torr. The current modifications involved making the flow tube of modular design with separate source, reaction, and detection regions. The detection region consists of a rectangular stainless steel block bored out internally to a two-inch circular cross-section and fitted with an internal Teflon® sleeve to retard surface recombination of atomic species. The block contains two viewing positions placed 7.5 cm apart. Each viewing position has a circular port on each of the four faces of the block which can accommodate resonance lamps, a vacuum ultraviolet monochromator or transfer optics for the observation of emissions within the flow tube by an external uv/visible/infrared monochromator. Currently, the upstream observation position is outfitted with two microwave-discharge resonance lamps placed normal to each other, and a 0.2-m vacuum ultraviolet monochromator (Minuteman 302 VM) diametrically opposite one of the resonance lamps. The lamp which is viewed by the monochromator is used in absorption studies, while the lamp normal to the monochromator's optical axis is used to excite resonance fluorescence of atomic species formed in the flow reactor. The lamps and the monochromator are separated from the flow tube by 25 mm diameter $MgF_2$ windows which have a short wavelength cutoff of 115 nm. In addition, a $MgF_2$ lens in the optical train of the monochromator collects light from the flow tube.

A schematic showing the resonance lamps and detection cell is given in Fig. 3. The lamps are constructed from 13 mm (o.d.), medium-wall Pyrex®

tubing. He or Ar flow through each lamp at rates of ~ 150 μmol $s^{-1}$ and total pressures of ~ 2 torr. The discharge plasmas are excited by Evenson[17] cavities powered by 2.45 GHz supplies (Raytheon PGM-10) operating at power settings of 10-20 W. If one does not employ sound vacuum techniques, including scrupulous cleaning of the components, with special attention to the portions in and upstream of the active discharge, variations in lamp intensity and emitter line width often will occur due to leaks and outgassing. In addition it is important to construct the lamp so that the gas flow enters near the window and passes from front to back, and to position the discharge cavity so that the plasma extends to the front window. This procedure inhibits the buildup of pockets of absorbing atoms between the emitting region and the exit window. Although controlled amounts of $N_2$ can be added to the lamp, the impurity level of $N_2$ (i.e., a few ppm) in the He and Ar bath gases is sufficient to give intense but optically thin multiplets at 149 and 174 nm. The absence of self-absorption is determined spectrally by confirming that the observed intra-multiplet line ratios are consistent with those predicted from spin-orbit sum rules.[18] Instability in the emission intensity, due to long-term variations in the lamp cooling rate and thereby in the steady-state operating temperature of the lamp (typically 500-600 K), is minimized by regulating the flow of cooling air to the cavity.

Atomic nitrogen metastables are made in the flow tube by discharging mixtures of nitrogen and argon in a McCarroll[19] cavity powered by another Raytheon 2.45 GHz supply. Molecular nitrogen is moderately efficient at quenching the atomic metastables ($k_{N(^2D)} + N_2 = 1.6 \times 10^{-14}$ $cm^3$ $molecule^{-1}$ $s^{-1}$),[14,20] so that the best metastable yields come from fairly dilute mixtures of $N_2$ in Ar, typically $\leq 1\%$ $N_2$ at total gas flows of 2-5 x $10^3$ μmol $s^{-1}$, total pressures of 1-5 torr, and linear flow velocities of 1-2 x $10^3$ cm $s^{-1}$.

Reagents such as NO or $CO_2$, for use in titration experiments to determine atom densities, are injected into the flow tube through a one-inch diameter loop constructed from 2 mm o.d. polyethylene tubing, with numerous small holes around both the inside and outside surfaces of the loop. The loop is presently situated about 30 cm upstream of the observation region, but this distance can be increased as necessary by adding a section of flow tube of

the desired length between the section containing the reagent inlet and that containing the detector head. In addition, mixing times for a fixed injection position can be varied over a wide range by altering the amount of throttling of the pump on the flow tube, thereby reducing or increasing the gas flow velocity. The nitrogen metastable number density is not significantly affected by this procedure, because throttling the pump simultaneously increases the flow tube pressure and reduces the pumping speed at fixed total gas flow. The primary loss mechanism for the metastables is diffusion to the reactor walls, and although reducing the flow velocity gives the metastables more time in which to diffuse, the simultaneous increase in the total pressure decreases the rate at which the metastables diffuse to the walls, thus resulting in a cancellation effect.

## 4. LAMP EXCITATION MECHANISMS

A variety of different line excitation mechanisms in resonance discharge lamps can be proposed which involve collisions of electrons or bath gas metastables with a parent species, either atomic, molecular, or ionic. However, in most cases, the only two important excitation mechanisms likely to obtain in low power microwave or radio frequency discharges will be electron impact excitation of the parent atom, or rare-gas metastable energy transfer. The latter mechanism is likely to involve dissociative excitation of the parent molecule by helium metastables in a helium lamp, and direct energy transfer between metastable argon and the parent atom in an argon lamp. Electron impact excitation will impart very little kinetic energy to the excited atom, thus giving Doppler-broadened emission line widths which are determined primarily by the lamp bath-gas temperature. In contrast, the rare-gas metastable excitation often includes considerable transfer of excess kinetic energy to the excited atoms, thus giving Doppler broadened lines which are much larger than those determined by the local translational temperature. In this paper we will focus on OI (130 nm) and NI (120, 149, and 174 nm) although some information is also available on H,[15,21] Cl,[22] Br,[13] I[23] and Kr[24] lamps.

Problems associated with non-thermal broadening processes in atomic resonance lamps were probably first noticed by Lin, Parkes and Kaufman[14, 25] who studied atomic oxygen absorption at 130 nm using microwave powered lamps with both argon and helium bath gases. They noticed that the oscillator strength deduced from their data for the 130 nm transition was a factor of two larger if they used a helium lamp rather than an argon lamp to excite the radiation. Later, Piper[8a] showed that the electronic energy transfer reaction between metastable argon and atomic oxygen was efficient and excited the 3p $^3P$ state of atomic oxygen which was 0.56 eV below the energy of the metastable argon. The 3s $^3S$ state of atomic oxygen, which is the upper state of the 130 nm radiation, is populated by radiative cascade at 844.6 nm from the 3p $^3P$ state. Further experiments by Piper, Clyne and Monkhouse[8b] showed that the rate constant for excitation of the 3s $^3S$ state of atomic oxygen in the Ar* + O interaction is almost gas kinetic ($8.2 \times 10^{-11}$ $cm^3$

molecule$^{-1}$ s$^{-1}$), and that furthermore, absorption studies on the 130 nm radiation produced in the Ar* + O reaction require an effective Doppler temperature of 3400 K for the 130 nm emission in order to reproduce the well known 130 nm oscillator strength.[11] The deduced kinetic temperature implies a translational energy in the excited oxygen of 0.44 eV, which agrees quite well with the 0.4 eV expected on the basis of the 0.56 eV exoergicity of the Ar*/O interaction. A reanalysis of the argon lamp data of Lin et al.[26] shows that the effective temperature in their lamp was about 2500 K, in modest accord with the energy transfer studies of Piper et al.[8] This clearly shows that the major excitation pathway in the Ar/O microwave lamp is the energy transfer reaction between metastable argon and atomic oxygen. A modest amount of electron impact excitation must also obtain in the lamp to account for the lower effective 130 nm temperature in the lamp compared to the energy transfer studies.

Piper and Clyne[7] have shown that the dissociative excitation of molecular oxygen by metastable helium produces the 130 nm transition of atomic oxygen with effective temperatures greater than 4000 K. The effective emitter temperature was reduced markedly as the pressure in their $He^*/O_2$ source was increased from 1 to 6 torr. They explained this behavior in terms of collisional moderation of the excited atomic oxygen atoms prior to emission. Since the lifetime of the 3s $^3S$ state is only 2 ns,[11] much shorter than the time between collisions at a few torr, the atomic oxygen must be excited in part via radiative cascade from longer lived, higher lying states of the triplet manifold. Chang, Setser and Taylor[27] surveyed the emission from the various atomic oxygen states produced in the dissociative excitation of molecular oxygen by metastable helium and confirmed that significant excitation does occur to higher levels in the oxygen triplet manifold. In addition, they ascertained that the rate constant for excitation of the 3s $^3S$ state, including both direct and cascade excitation, in the $He^*/O_2$ reaction is $1.8 \times 10^{-11}$ cm$^3$ molecule$^{-1}$ s$^{-1}$.

Rawlins and Kaufman[6] used resonance absorption techniques to study oxygen lamps containing helium bath gas. They noticed a strong increase in the effective 130 nm linewidth with decreasing lamp power and with decreasing

lamp pressure. They estimated that if dissociative excitation of molecular oxygen by metastable helium proceeded with a rate constant of about $10^{-11}$ $cm^3$ $molecule^{-1}$ $s^{-1}$ or faster that the metastable excitation pathway could compete effectively with direct electron impact excitation of atomic oxygen. It is interesting that a lamp which appears to behave quite normally at moderate power levels and pressures shows drastically different behavior at low power and pressure. These results clearly illustrate that an understanding of lamp excitation mechanisms is crucial to the determination of appropriate lamp operating conditions.

While nitrogen resonance lamps have not been studied in such great detail as atomic oxygen lamps, some information on lamp operation and on energy transfer studies is available. In their study of the $He^*/N_2$ interaction, Chang et al.[27] failed to observe any significant atomic radiation, thus casting doubt upon dissociative excitation of molecular nitrogen by metastable helium as a viable excitation mechanism in $He/N_2$ lamps. This finding is further supported by the fact that, in contrast to $O_2$/He lamps, only the $He(^1S)$ state (20.6 eV) can dissociatively excite NI transitions; the population of this state in the plasma will be smaller than that of the $He(^3S)$ state (19.8 eV) which is important in OI excitation. By analogy with the $He^*/O_2$ case, we anticipate that the dissociative excitation pathway is slow relative to electron impact and, furthermore, that the degree of broadening is relatively small due to the low exoergicity of the process (0.6 eV for 120 nm, 0.15 eV for 149 and 174 nm).

We therefore expect that the effective emitter temperature in nitrogen lamps containing helium bath gas will be determined primarily by the effective translational temperature in the discharge plasma. This seems to be the case for the 120 nm transition ($2p^2 3s\ ^4P - 2p^3\ ^4S$) of atomic nitrogen, where oscillator strengths of that transition measured in line absorption studies using the mean translational temperature of the plasma (as determined from pressure increase upon igniting the discharge or rotational temperatures of diatomic emitters in the plasma) are in good agreement with direct lifetime measurements of the same transition.[6,25,28]

The case for Ar discharges is more difficult to interpret. Piper et al.[29] have studied the transfer of electronic energy from metastable argon to atomic nitrogen. They determined rate constants for excitation of the 3s $^2$P and 3s $^4$P states of NI by metastable argon to be 9.0 and 1.6 x $10^{-11}$ $cm^3$ $molecule^{-1}$ $s^{-1}$, respectively. If the energy transfer reaction between metastable argon and atomic nitrogen excites the $^2$P and $^4$P levels of atomic nitrogen directly, an exoergicity of 0.87 and 1.21 eV, respectively would accompany the energy transfer. Such exoergicities imply a translational energy in the excited nitrogen atoms of 0.64 and 0.90 eV for the $^2$P and $^4$P states, respectively. However, there are slightly endoergic reaction channels (i.e., endoergic by less than 2kT at 300 K) through which the energy transfer process could occur, so it is not obvious that the atomic nitrogen lines emitted in the Ar/N lamp will be broadened at all.

In the present experiments we have begun to characterize experimentally lamps for use in absorption studies on metastable nitrogen atoms, N($^2$D, $^2$P), for which the diagnostic emissions emanate from a common upper state, 3s $^2$P, with wavelengths of 149 and 174 nm, respectively (cf. Table I). Absorption measurements have been made on both the 149 and 174 nm multiplets with constant number densities of N($^2$D) and N($^2$P), using both helium and argon lamps. These measurements indicate that the ratio of $A^{He}/A^{Ar} \simeq 2.0$ and 2.3 for the 149.3 and 174.3 nm lines, respectively. Assuming that the translational temperature of the excited atoms giving rise to the 149.3 and 174.3 nm emission in the helium lamp is 600 K[6,25] (i.e., following the reasoning outlined above) then application of Eqs. (9) and (10) to the above results indicates a translational temperature of 3300 K and 4500 K in the argon lamp for the absorption measurements on the 149.3 and 174.3 nm lines, respectively. Since the maximum absorbance of the 174.3 nm line was almost a factor of three smaller than that for the 149.3 nm line, the approximation of Eq. (9) should be more applicable to absorptions on the longer wavelength multiplet. The mean translational energy implied by a kinetic temperature of 4500 K is 0.58 eV, which is reasonably close to the value of 0.64 eV expected if the 3s $^2$P state of atomic nitrogen is excited directly by collisions between metastable Ar($^3P_2$) and N($^4$S) in the argon lamp.[7] In order to characterize the lamp behavior more precisely, it

will be necessary to measure absorptions for both lamps as a function of metastable nitrogen number density and to determine the actual translational temperature in the helium lamp. This latter measurement can be made most easily by measuring the rotational temperature of OH in the lamp when a trace of $H_2O$ is introduced into the helium flow upstream of the discharge. The OH rotational temperature and bath gas translational temperature should be equal. The metastable $N(^2D)$ number density can be varied and determined absolutely by titration reactions with $CO_2$, $N_2O$, or $O_2$ to form NO, which is in turn converted rapidly to $O(^3P)$ by reaction with $N(^4S)$ in the gas stream. $O(^3P)$ number densities, which can be determined by resonance fluorescence, can be related quantitatively to $N(^2D)$ number densities using the known kinetics of the system.[20] These measurements are currently being pursued.

We investigated the possibility of modifying the excitation mechanisms in the argon lamp to enhance excitation by electrons relative to that by metastable argon thus narrowing the effective linewidth at 149 and 175 nm. Xenon in varying number densities was added to the argon flow. Xenon is known to be a rapid quencher of metastable argon with a quenching rate constant of $1.8 \times 10^{-10}$ $cm^3$ $molecule^{-1}$ $s^{-1}$.[30] The long-lived metastable energy levels of xenon which are produced by a radiative cascade process in the transfer of energy between $Ar(^3P_2)$ and Xe[31] are too low in energy to excite the 3s $^2P$ level on atomic nitrogen in an energy-transfer reaction. The results of the experiments showed no change in absorbance at 149.3 nm by the metastable $N(^2D)$ even at xenon number densities as high as $3 \times 10^{15}$ atoms $cm^{-3}$. We had anticipated that the absorbance at 149.3 nm for a constant $[N(^2D)]$ would increase as the electron excitation branch became a more significant fraction of the total N 3s $^2P$ excitation. The intensity of the 149.3 nm line was reduced by a factor of five at the maximum xenon number density, indicating that some quenching of the metastable argon by the xenon was taking place, but clearly that amount of quenching was not sufficient to alter the primary excitation mechanism in the lamp.

Our observation of extensive broadening from direct excitation of the 149 and 174 nm transitions by Ar* is in marked contrast to other results for the 120 nm transition. Lin et al.[25] noticed no difference between the oscillator strength for the 120 nm transition deduced from absorption measurements

using an argon lamp and those deduced using a helium lamp. This indicates that either (1) the electron impact excitation mechanism is dominant in the argon lamp for 120 nm excitation, or (2) the 120 nm excitation by metastable argon is indirect, via the slightly endoergic, radiative cascade route. The 120 nm excitation rate constant measured by Piper et al.[29] is lower by a factor of 5-6 than the rate constants for excitation of the 130 nm transition via Ar* + O or of the 149 nm/174 nm transitions via Ar* + N, both of which produce broadened emission lines in argon plasmas. Furthermore, the effective rate coefficient for electron impact excitation of atomic nitrogen is over an order of magnitude larger for 120 nm than for 149 and 174 nm.[32] Thus it appears that electron impact is the dominant excitation pathway for 120 nm emission, regardless of the Ar* + N mechanism.

In conclusion, we have described how collisional energy transfer processes involving rare gas metastables can excite atomic resonance transitions and, furthermore, can give rise to non-thermal Doppler broadening of the lines. We have used the framework of resonance absorption theory to interpret the effects of these processes for the available data on OI and NI resonance multiplets in He and Ar discharges, and have presented new experimental data exhibiting direct excitation of NI (149 nm, 174 nm) radiation by metastable argon. This body of results clearly illustrates the importance of careful consideration of lamp excitation mechanisms and characterization of line broadening effects in the design and interpretation of resonance absorption/fluorescence measurements.

ACKNOWLEDGEMENTS

Portions of this research were performed at the Air Force Geophysics Laboratory, Bedford, MA, under ESD/AFSC Contract F19628-80-C-0174, with support from the Air Force Office of Scientific Research and the Defense Nuclear Agency. We are grateful to R. A. Armstrong and J. P. Kennealy (AFGL) for use of the discharge-flow facility, and to H. C. Murphy (PSI) for assistance with the design modifications. G. E. Caledonia (PSI) participated in useful discussions.

## REFERENCES


1. See, for example, a) B. A. Ridley, J. A. Davenport, L. J. Stief, and K. H. Welge, J. Chem. Phys. 57, 520 (1972); b) P. P. Bemand and M. A. A. Clyne, Chem. Soc. Faraday Trans. II 69, 1643 (1973); c) P. Roth and Th. Just, Berichte Bunsengesellshaft 81, 572 (1977); and references cited below.

2. a) D. Davis and W. Braun, "Intense Vacuum UV Line Sources," Appl. Opt. 7, 2071 (1968); b) W. Braun and T. Carrington, "Line Emission Sources for Concentration Measurements and Photochemistry," J. Quant. Spectrosc. Radiat. Transfer 9, 1133 (1969).

3. P. H. G. Dickinson, W. C. Bain, L. Thomas, E. R. Williams, D. B. Jenkins, and N. D. Twiddy, "The Determination of the Atomic Oxygen Concentration and Associated Parameters in the Lower Ionosphere," Proc. R. Soc. Lond. A 369, 379 (1980).

4. J. G. Anderson, "The Absolute Concentration of $O(^3P)$ in the Earth's Stratosphere," Geophys. Res. Lett. 2, 231 (1975).

5. T. M. Donahue, J. G. Anderson, W. T. Rawlins, F. Kaufman, and R. D. Hudson, "Apollo-Suyuz $O(^3P)$ and $N(^4S)$ Density Measurement by UV Spectroscopy," Geophys. Res. Lett. 4, 79, (1977).

6. W. T. Rawlins and F. Kaufman, "Characteristics of O(I) and N(I) Resonance Line Broadening in Low Pressure Helium Discharge Lamps," J. Quant. Spectrosc. Radiat. Transfer 18, 561, (1977).

7. L. G. Piper and M. A. A. Clyne, "Translational Energy of $O(3S\ ^3S)$ Excited by the Dissociative Excitation of $O_2$ and NO by $He^*(2\ ^3S)$," Chem. Phys. submitted (1981)

8. a) L. G. Piper, "Electronic Energy Transfer Between Metastable Argon Atoms and Ground-state Oxygen Atoms," Chem. Phys. Lett. 28, 276 (1974); b) L. G. Piper, M. A. A. Clyne and P. B. Monkhouse, "Electronic Energy Transfer from Metastable $Ar(^3P_{2,0})$ to Ground State $O(^3P_J)$," manuscript in preparation.

9. J. P. Kennealy, F. P. Del Greco, G. E. Caledonia, and W. T. Rawlins, "COCHISE: Laboratory Spectroscopic Studies of Atmospheric Phenomena with High-sensitivity Cryogenic Instrumentation," SPIE 191, 151 (1979).

10. A. C. G. Mitchell, M. W. Zemansky, Resonance Radiation and Excited Atoms, Cambridge: The University Press (1934).

11. M. A. A. Clyne and L. G. Piper, "Kinetic Spectroscopy in the Far Vacuum Ultra-violet, Part 3," JCS Faraday II 72, 2178 (1976).

12. J. Tellinghuisen and M. A. A. Clyne, "Role of Hyperfine Structure in Atomic Absorption: Oscillator Strengths in Br and I," JCS Faraday II 72, 783 (1976).

13. M. A. A. Clyne and D. J. Smith, "Non-reversed Source of Br Atom Resonance Radiation and its Application to the Measurement of Br Atom Concentrations," JCS Faraday II 74, 263 (1978).

14. F. Kaufman and D. A. Parkes, "Sources of Error in Using Resonance Light Absorption to Measure Atomic Concentrations," Trans. Faraday Soc. 66, 1579 (1970).

15. a) M. A. A. Clyne, P. B. Monkhouse, "Energy Transfer in Collisions of Ar($^3P_{0,2}$) Metastable Atoms with H($^2S$) Atoms. I. Total Rate Constant and Mechanism," Chem. Phys. 28, 447 (1978); b) M. A. A. Clyne, M. C. Heaven, K. D. Bayes, and P. B. Monkhouse, "Energy Transfer in Collisions of Excited Ar($^3P_{0,2}$) Metastable Atoms with H($^2S$) Atoms. II. Lyman-α Emission Profile," Chem. Phys. 47, 179 (1980).

16. L. G. Piper and G. E. Caledonia, "Rate Constants for Deactivation of $N_2(A)v' = 0,1$ by $O_2$," J. Chem. Phys. 74, 2888 (1981).

17. F. C. Fehsenfeld, K. M. Evenson and H. P. Broida, "Microwave Discharge Cavities Operating at 2450 MHz," Rev. Sci. Instr. 36, 294 (1965).

18. C. Lin and F. Kaufman, "Reactions of Metastable Nitrogen Atoms," J. Chem. Phys. 55, (1971).

19. B. McCarroll, "An Improved Microwave Discharge Cavity for 2450 MHz," Rev. Sci. Instr. 41, 279 (1970).

20. D. Husain, S. K. Mitra, and A. N. Young, "Kinetic Study of Electronically Excited Nitrogen Atoms, N($2^2D_J$, $2^2P_J$), by Attenuation of Atomic Resonance Radiation in the Vacuum Ultra-violet," JCS Faraday II 70, 1721 (1974).

21. a) A. Lifshitz, G. B. Skinner, and D. R. Wood, "Resonance Absorption Measurements of Atom Concentrations in Reacting Gas Mixtures. I. Shapes of H and D Lyman-α Lines from Microwave Sources," J. Chem. Phys. 70, 5607 (1979); b) C. Chiang, A. Lifshitz, G. B. Skinner, and D. R. Wood, "Resonance Absorption Measurements of Atom Concentrations in Reacting Gas Mixtures. II. Calibration of Microwave Sources Over a Wide Temperature Range," J. Chem. Phys. 70, 5614 (1979).

22. M. A. A. Clyne and W. S. Nip, "Study of Elementary Reactions by Atomic Resonance Absorption with a Non-reversed Source, Part 2.-Oscillator Strengths for Cl 4s-$3p^5$ Transitions and Rate Constants for Specific Product Channels from Ar($^3P_{2,0}$) + Cl," JCS Faraday II 73, 161 (1977).

23. M. A. A. Clyne and L. W. Townsend, "Determination of Atomic Oscillator Strengths using Resonance Absorption with a Doppler Line Source: Transitions of Br and I $(n + 1)s - np^5$," JCS Faraday II 70, 1863 (1974).

24. L. G. Piper, D. W. Setser, M. A. A. Clyne, "Electronic Energy Transfer from Metastable Argon Atoms to Krypton Atoms," J. Chem. Phys. 63, 5018 (1975).

25. C. Lin, D. A. Parkes, and F. Kaufman, "Oscillator Strength of the Resonance Transitions of Ground-State N and O," J. Chem. Phys. 53 3896 (1970).

26. L. G. Piper, unpublished results, Univ. of Pittsburgh (1975).

27. R. S. F. Chang, D. W. Setser, and G. W. Taylor, "Assignment of Rate Constants to Exit Channels from Quenching of $He(2\ ^3S)$ Metastable Atoms," preprint (1978).

28. M. A. A. Clyne, S. Jaffe, and P. D. Whitefield, "Kinetic Spectroscopy in the Far Vacuum Ultraviolet, Part 5-Oscillator Strengths for the 3s, 4s, 5s, 3d and 4d $^4P_J - 2p^3\ ^4S^0_{\frac{3}{2}}$ Transitions in Atomic Nitrogen," JCS. Faraday II 76 369(1980).

29. L. G. Piper, M. A. A. Clyne and P. B. Monkhouse, "Electronic Energy Transfer from Metastable Argon Atoms to Ground-state Nitrogen Atoms," Chem. Phys. 51, 107 (1980).

30. L. G. Piper, J. E. Velazco, and D. W. Setser, "Quenching Cross Sections for Electronic Energy Transfer Reactions Between Metastable Argon Atoms and Noble Gases and Small Molecules," J. Chem. Phys. 59 3323 (1973).

31. D. L. King, L. G. Piper, and D. W. Setser, "Electronic Energy Transfer from Metastable Argon $(4s\ ^3P_{2,0})$ to Xenon, Oxygen and Chlorine Atoms," JCS Faraday II 73, 177 (1977).

32. E. J. Stone and E. C. Zipf, "Excitation of Atomic Nitrogen by Electron Impact," J. Chem. Phys. 58 4278 (1973).

TABLE I.

Resonance Lines for Metastable Nitrogen Atoms

| Atom | Wavelength nm | Upper State | Lower State | $g_\ell$ | Relative Intensity | $f_{\ell_u}$ [a] |
|---|---|---|---|---|---|---|
| $N(^2D)$ | 149.2615 | $^2P_{3/2}$ | $^2D^\circ_{5/2}$ | 6 | 9 | 0.078 |
| | 149.2812 | $^2P_{3/2}$ | $^2D^\circ_{3/2}$ | 4 | 1 | 0.013 |
| | 149.4668 | $^2P_{1/2}$ | $^2D^\circ_{3/2}$ | 4 | 5 | 0.065 |
| $N(^2P)$ | 174.2717 | $^2P_{3/2}$ | $^2P^\circ_{3/2}$ | 2 | 1 | 0.021 |
| | 174.2725 | $^2P_{3/2}$ | $^2P^\circ_{3/2}$ | 4 | 5 | 0.053 |
| | 174.5246 | $^2P_{1/2}$ | $^2P^\circ_{1/3}$ | 2 | 2 | 0.043 |
| | 174.5255 | $^2P_{1/2}$ | $^2P^\circ_{3/2}$ | 4 | 1 | 0.011 |

a. Lawrence, G. M. and Savage, B. D., "Radiative Lifetimes of UV Multiplets in Boron, Carbon and Nitrogen," Phys. Rev. 141, 67(1966).

## FIGURE CAPTIONS

Fig. 1 Profiles of two Doppler-broadened lines of equal integrated intensity but different effective temperatures. This shows the poor overlap between lines of significantly different widths. The frequency units are from Eq. (3). For the 149.3 nm transition of NI one reduced frequency unit corresponds to 0.16 $cm^{-1}$ or 4.8 GHz. It corresponds to a wavelength increment of 0.36 pm.

Fig. 2 Diagram of the flow reactor illustrating the modular construction of the discharge head, reaction zone, detection cell, and the pumping port. Only the resonance absorption configuration is depicted here.

Fig. 3 Cross sectional view of the absorption/fluorescence cell showing the placement of the lamps. The direction of the flow in the reactor is perpendicular to the figure.

Fig. 4 Energy-level diagram of atomic oxygen showing the levels and transitions important to understanding the transfer of electronic energy from metastable $Ar(^3P_{2,0})$ to $O(^3P)$.

Fig. 5 Energy level diagram of atomic nitrogen showing the levels and transitions important to understanding the transfer of electronic energy from metastable $Ar(^3P_{0,2})$ to $N(^4S)$.

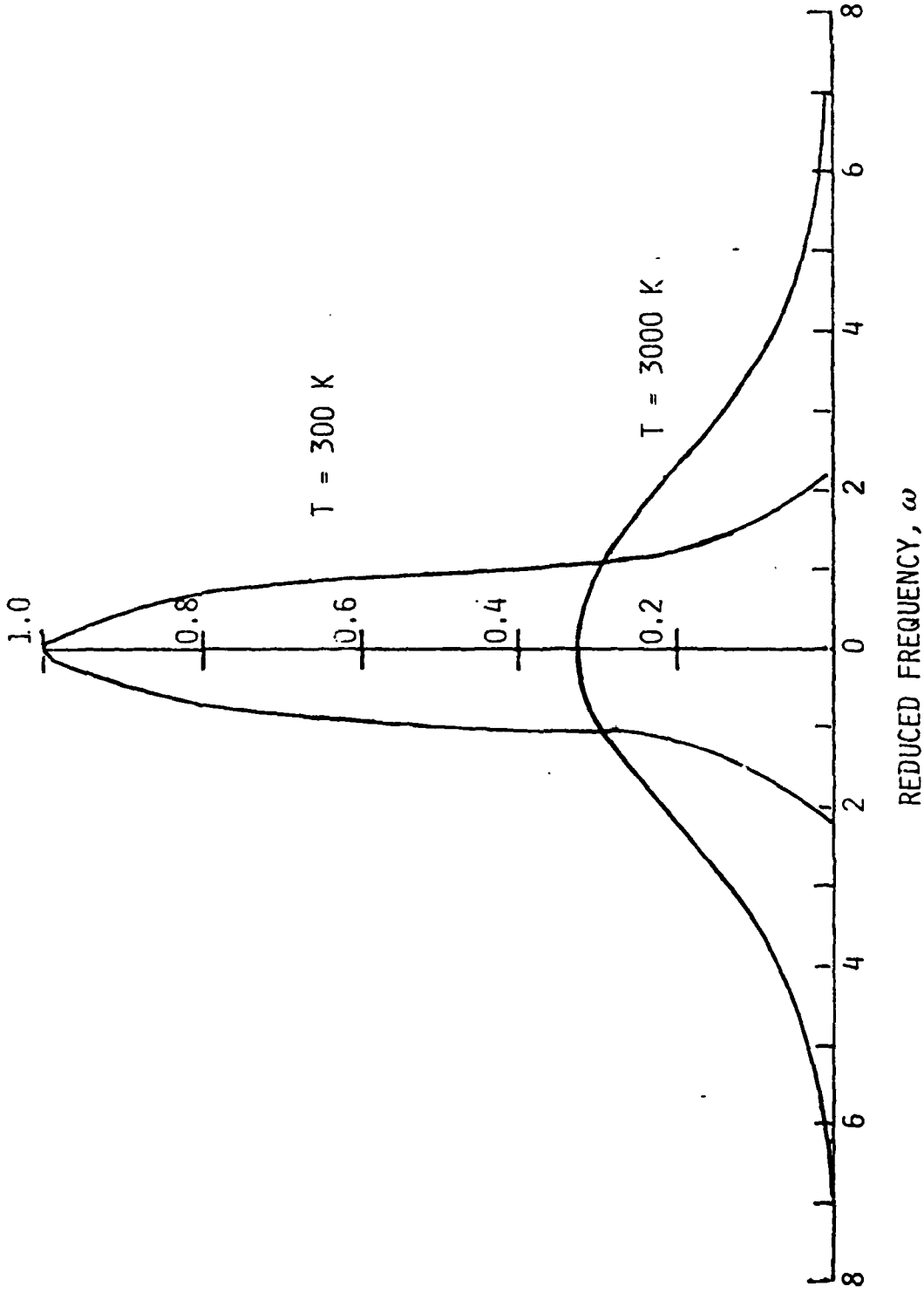


Fig. 1

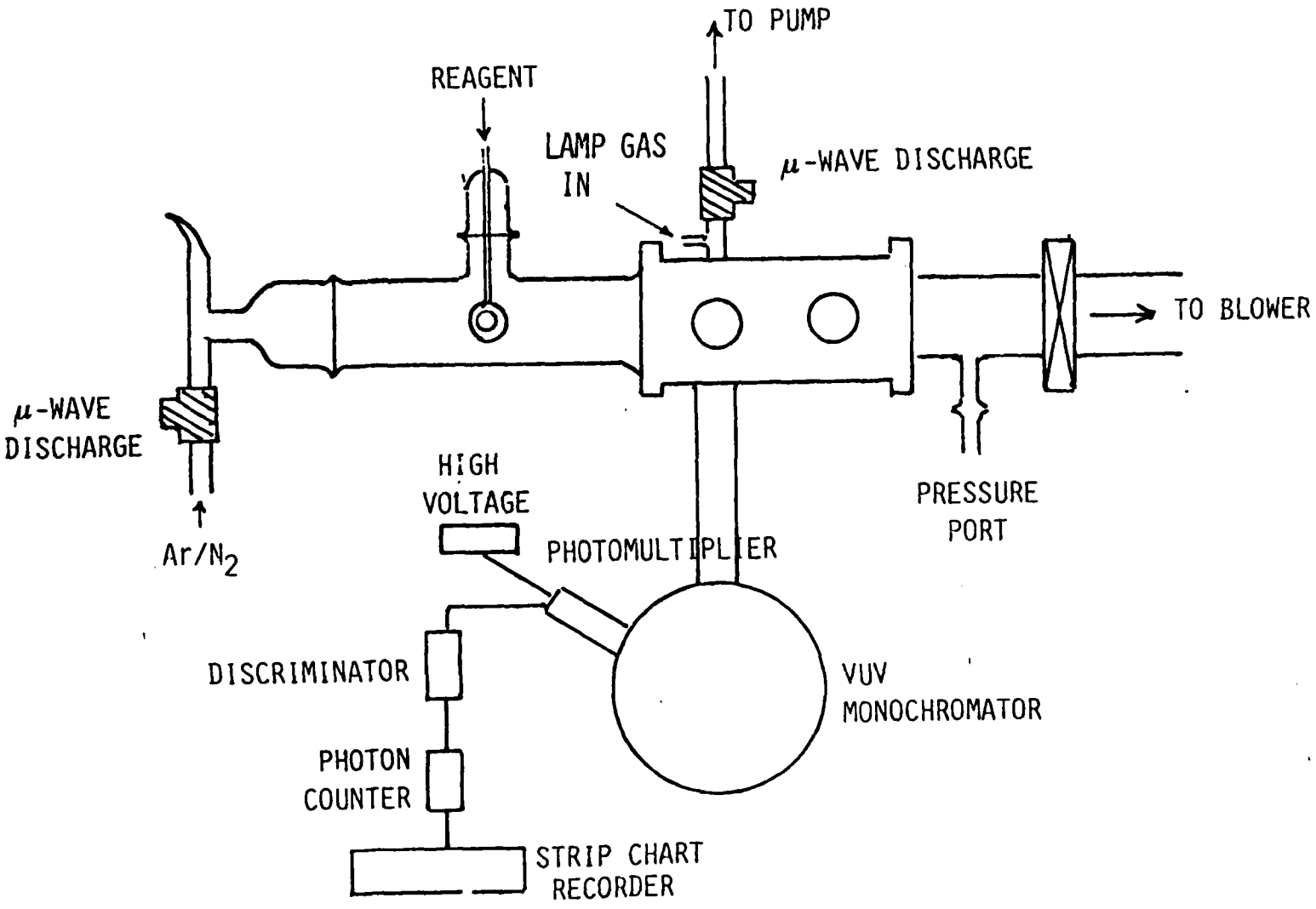
TO PUMP
REAGENT
LAMP GAS IN
μ-WAVE DISCHARGE
TO BLOWER
μ-WAVE DISCHARGE
HIGH VOLTAGE
PRESSURE PORT
Ar/N2
PHOTOMULTIPLIER
DISCRIMINATOR
VUV MONOCHROMATOR
PHOTON COUNTER
STRIP CHART RECORDER

Fig. 2

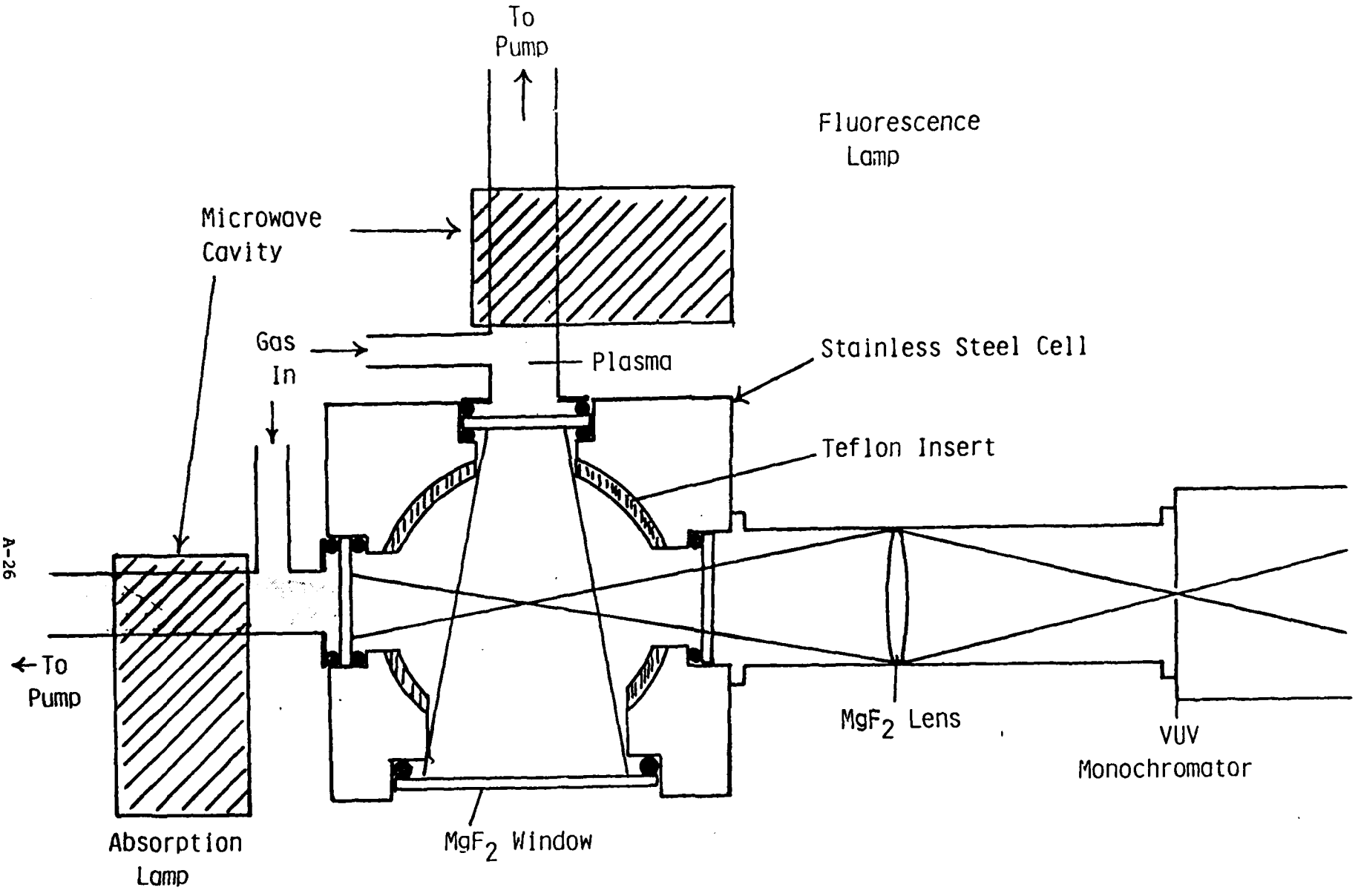
To
Pump
Fluorescence
Lamp
Microwave
Cavity
Gas
In
Plasma
Stainless Steel Cell
Teflon Insert
To
Pump
MgF2 Lens
VUV
Monochromator
Absorption
Lamp
MgF2 Window



Fig. 3

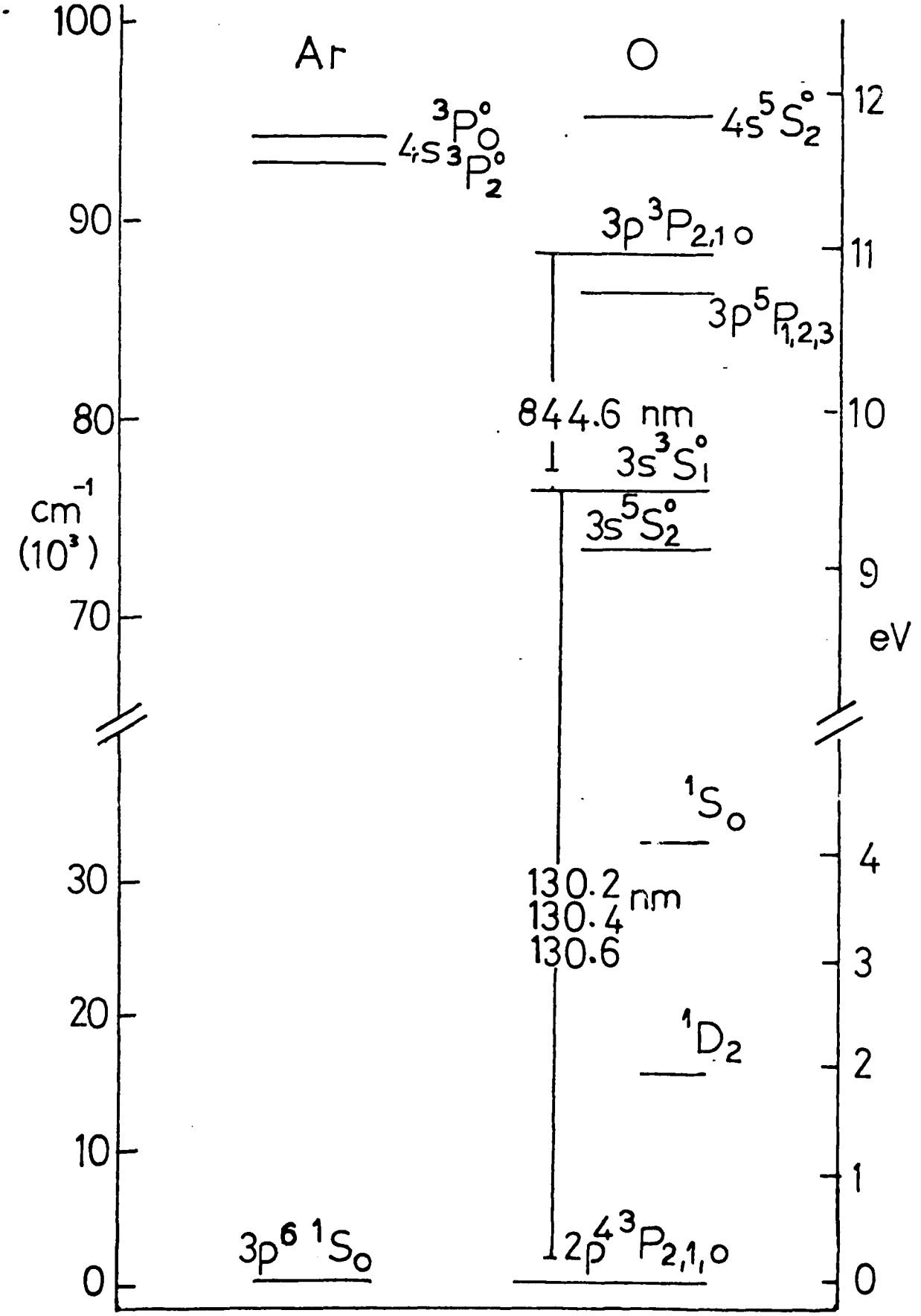
100
90
80
70
30
20
10
0
cm⁻¹
(10³)
Ar
O
3P°0
4s 3P°2
4s 5S°2
3p 3P2,1 o
3p 5P1,2,3
844.6 nm
3s 3S°1
3s 5S°2
1So
130.2 nm
130.4
130.6
1D2
3p6 1So
2p4 3P2,1,0
12
11
10
9
4
3
2
1
0
eV



Fig. 4

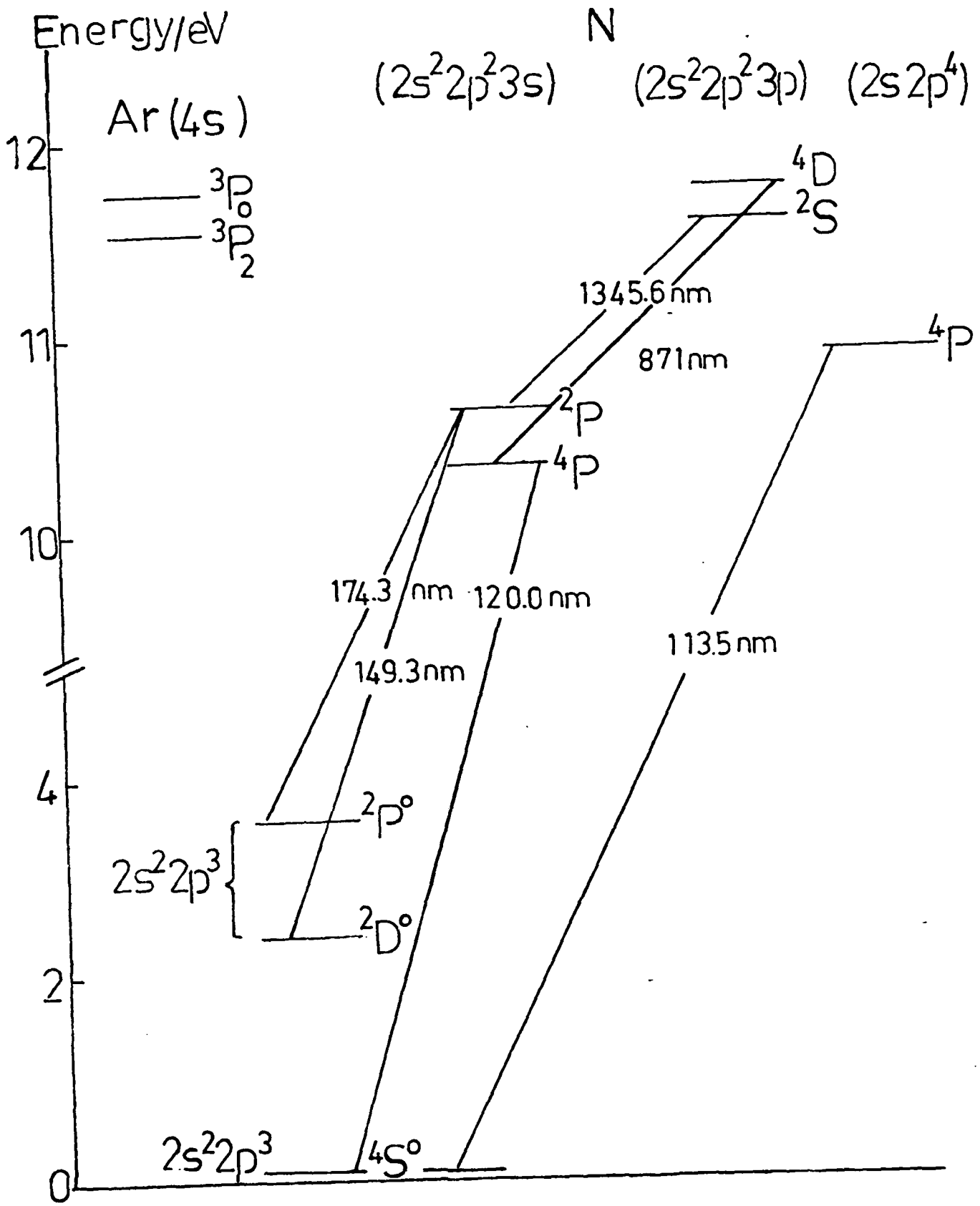
Energy/eV
N
(2s²2p²3s)
(2s²2p²3p)
(2s2p⁴)
Ar(4s)
12
11
10
4
2
0
³P₀
³P₂
⁴D
²S
⁴P
²P
⁴P
1345.6nm
871nm
174.3 nm
120.0 nm
149.3nm
113.5 nm
²P°
²D°
2s²2p³
2s²2p³
⁴S°

Fig. 5

# APPENDIX B

Design drawings of the component parts
of the COCHISE VUV diagnostic.

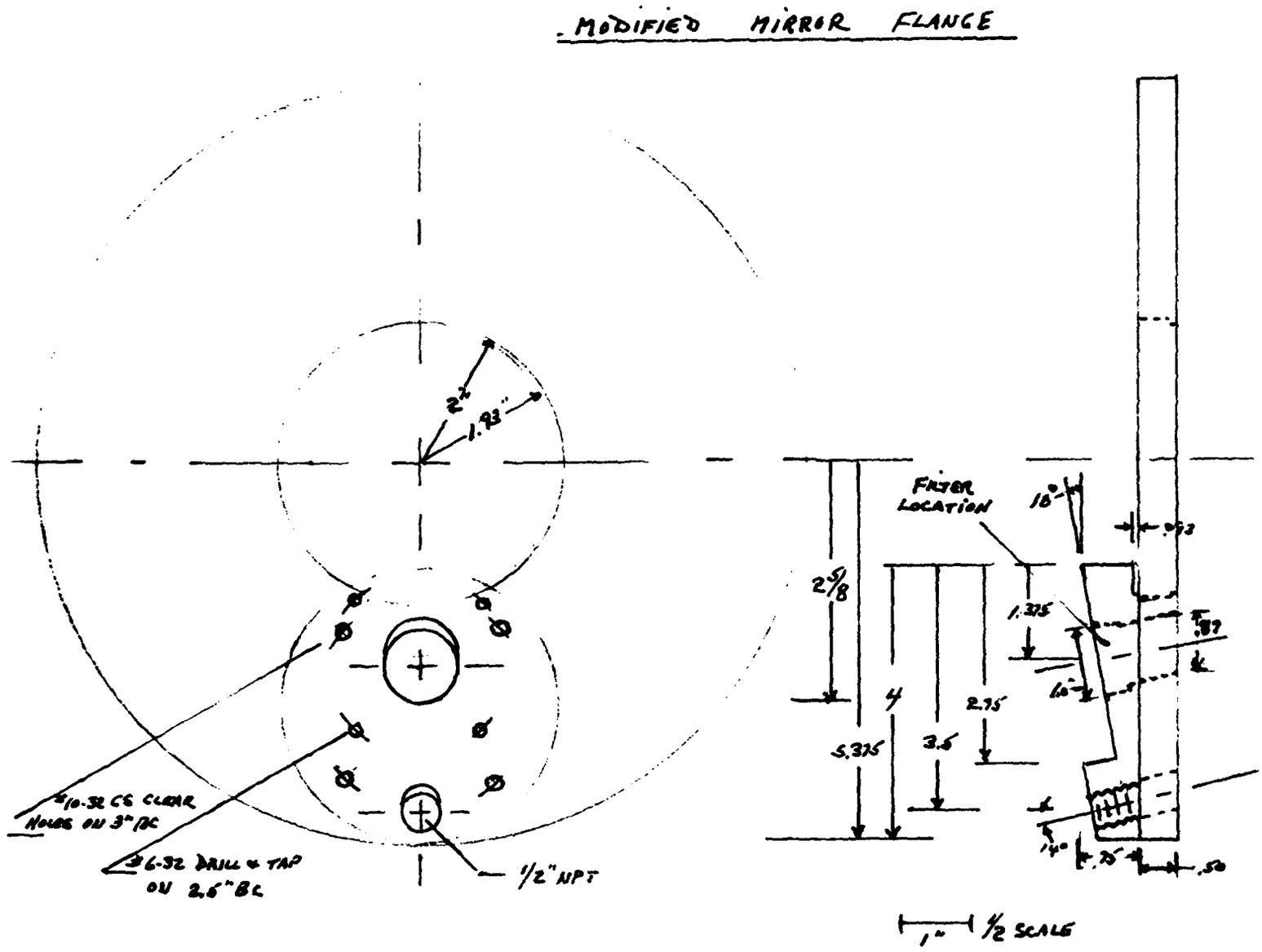


Fig. B-1 Mirror end of flange of COCHISE reaction cell modified to hold VUV lamp and detector.

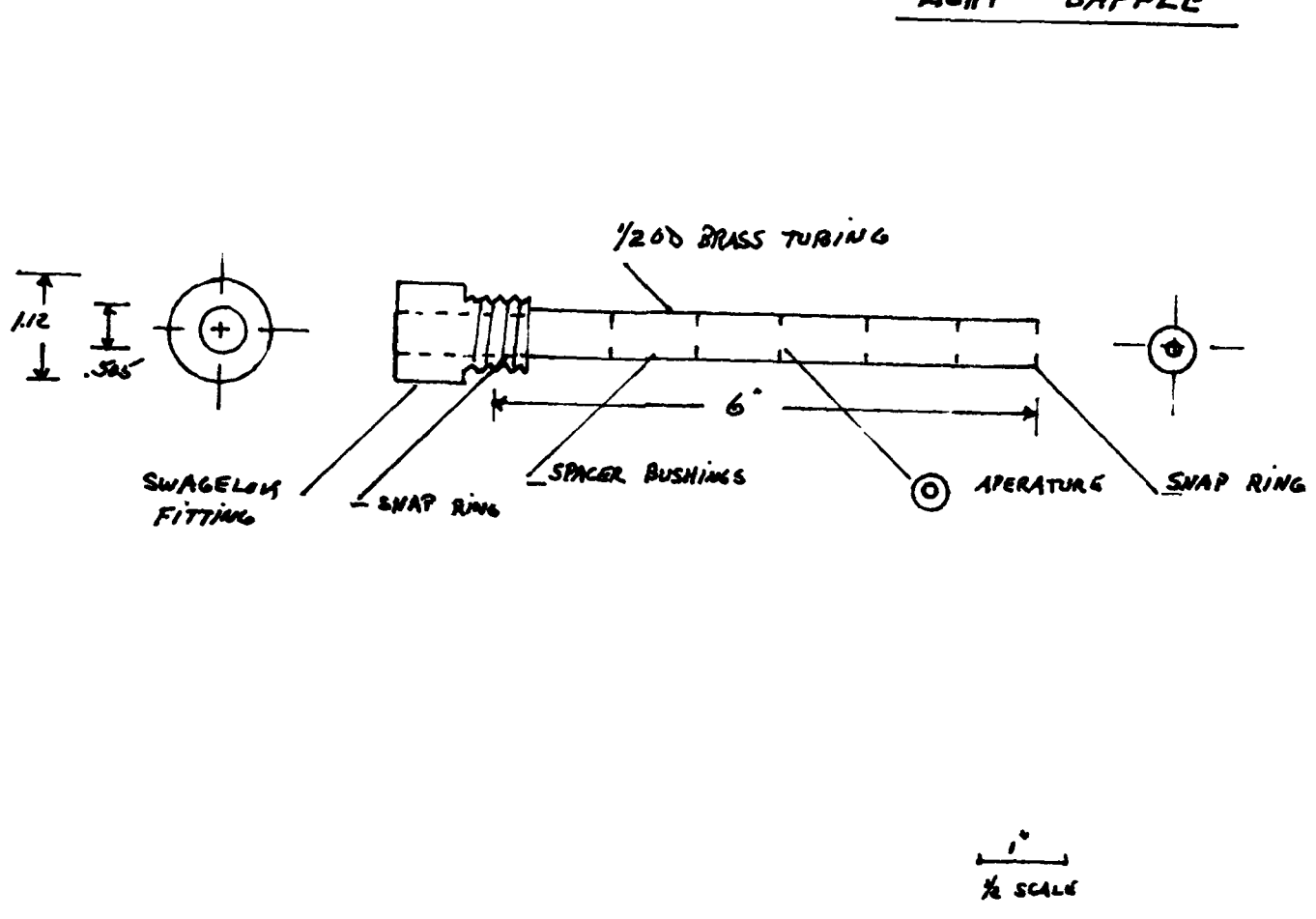


Fig. B-2 Baffel assembly for VUV lamp.

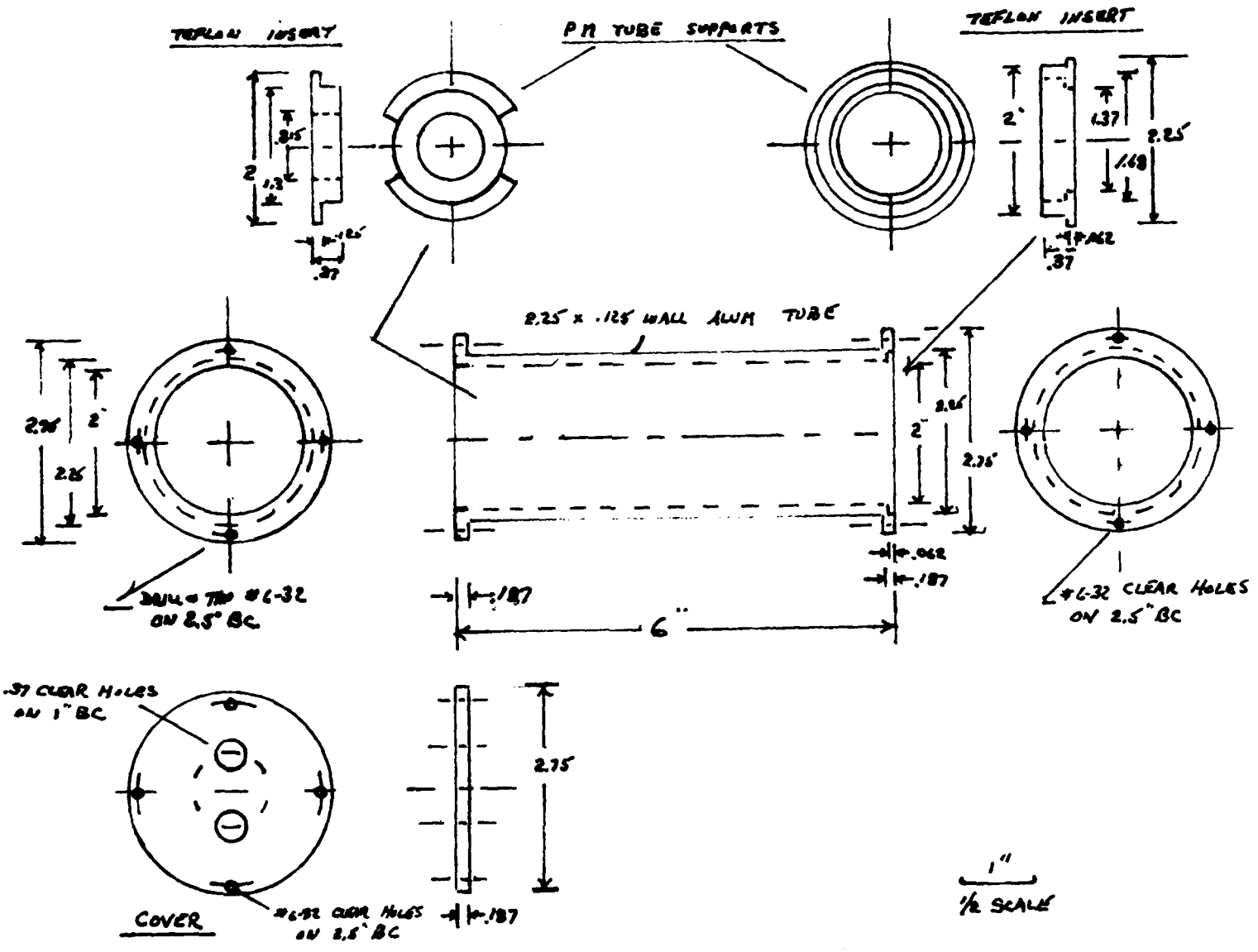


Fig. B-3 PMT housing for COCHISE VUV diagnostic.

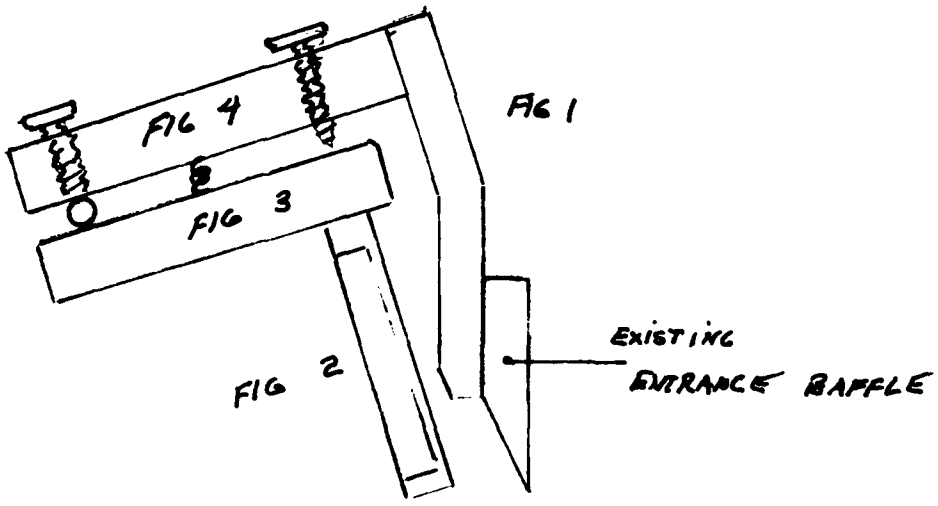


MIRROR MOUNT ASSEMBLY

1"
FULL SCALE

Fig. B-4 Mounting assembly for COCHISE VUV reflector.

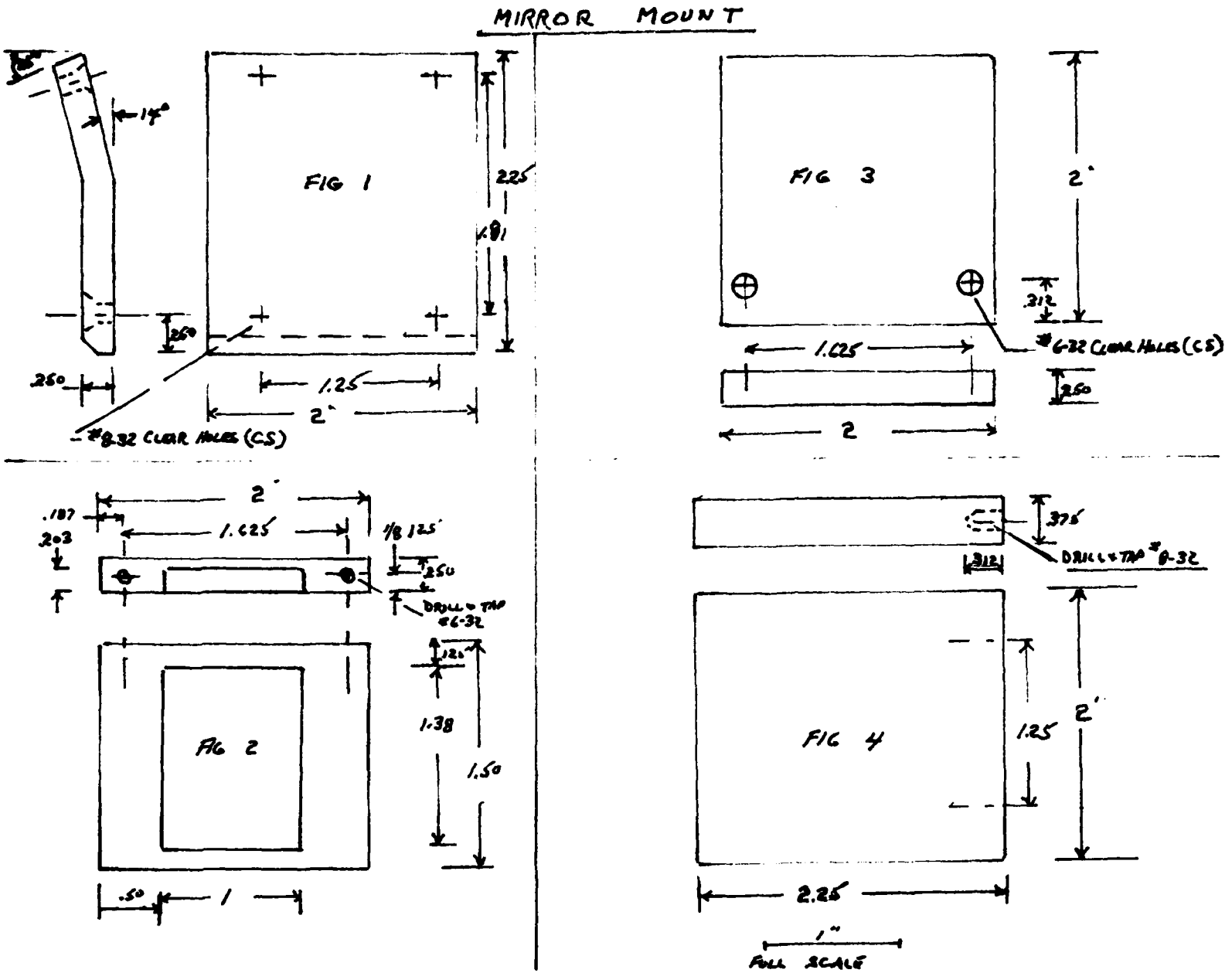


Fig. B-5 Component parts of COCHISE VUV reflector.